Organic & Biomolecular Chemistry

www.rsc.org/obc

Volume 7 | Number 21 | 7 November 2009 | Pages 4321–4548

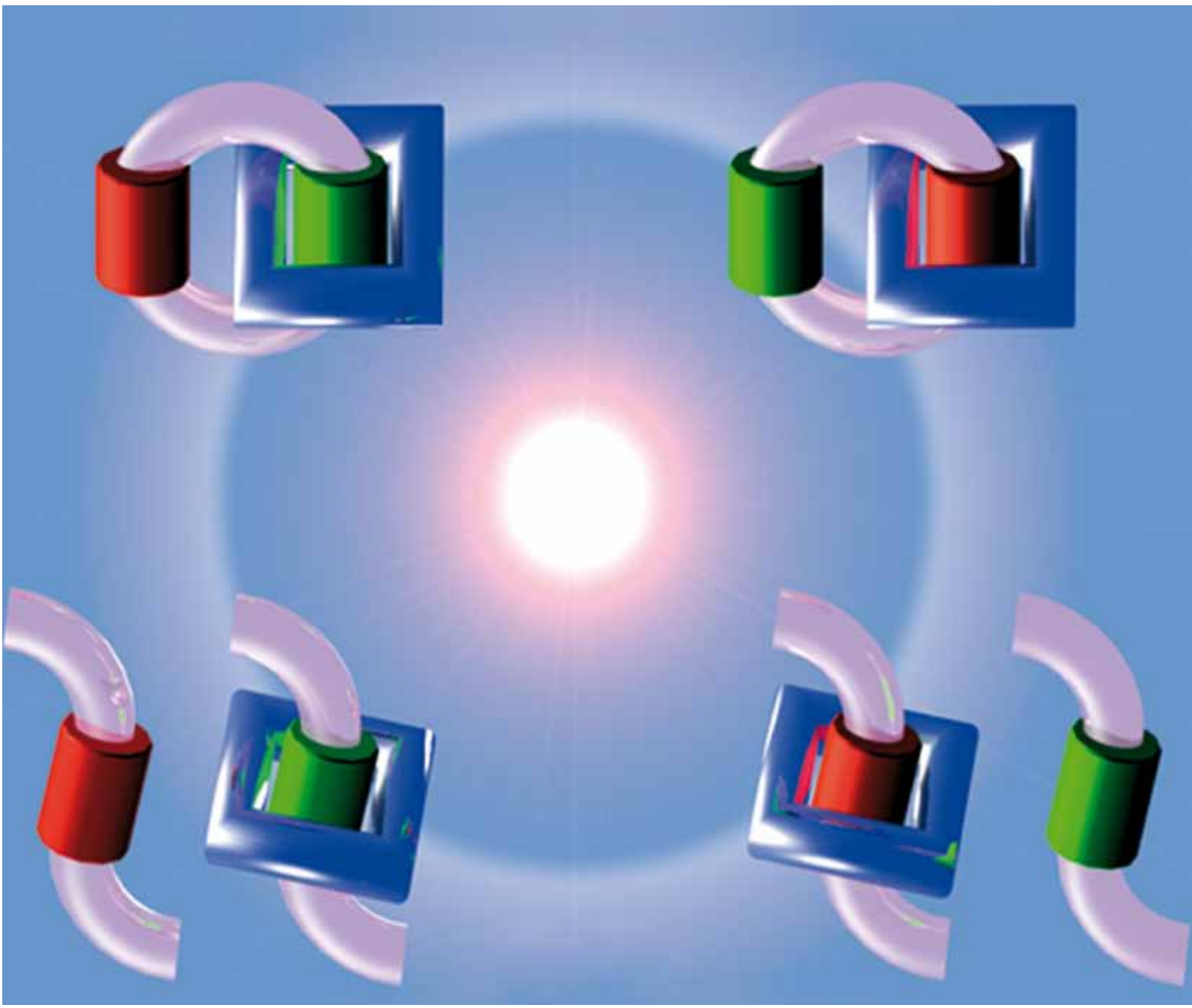

ISSN 1477-0520

RSC Publishing

FULL PAPER

J. Fraser Stoddart *et al.*

Thermodynamic forecasting of mechanically interlocked switches

Highlights in Chemical Biology

In this issue...

1477-0520(2009)7:21;1-D

Thermodynamic forecasting of mechanically interlocked switches†

Mark A. Olson,‡[a] Adam B. Braunschweig,‡[a] Taichi Ikeda,[b] Lei Fang,[a] Ali Trabolsi,[a] Alexandra M. Z. Slawin,[c] Saeed I. Khan[d] and J. Fraser Stoddart*[a]

Received 17th June 2009, Accepted 23rd July 2009
First published as an Advance Article on the web 3rd September 2009
DOI: 10.1039/b911874h

Mechanically interlocked molecular (MIM) switches in the form of bistable [2]rotaxanes and [2]catenanes have proven to be—when incorporated in molecular electronic devices (MEDs) and in nanoelectromechanical systems (NEMS)—a realistic and viable alternative to the silicon chip density challenge. Structural modifications and chemical environment can have a large impact on the relaxation thermodynamics of the molecular motions, such as translation and circumrotation in bistable rotaxanes and catenanes responsible for the operation of devices based on MIMs. The effects of structural modifications on the difference in free energy (ΔG°) for the equilibrium processes in switchable MIMs can be predicted by considering, firstly, the interactions present in their precursor pseudorotaxanes. By employing isothermal titration microcalorimetry (ITC) to investigate the thermodynamic parameters governing pseudorotaxane formation for a series of monosubstituted, acceptor host cyclophanes with various donor guests, in conjunction with X-ray crystallographic data, an obvious link between the noncovalent bonding interactions in pseudorotaxanes and MIMs that survive following the formation of the mechanical bond can be identified. It follows that the changes ($\Delta\Delta G^{\circ}$ values) in the difference of free energy during the formation of different pseudorotaxanes can subsequently be extrapolated to predict ΔG° values for the thermodynamics associated with switching in analogous MIM switches, employing the same donor–acceptor recognition components. In this manner, a systematic and predictive thermodynamic approach to designing and tuning switchable MIMs and MIM-based materials has been established. Additionally, these thermodynamic relationships are reminiscent of the long forgotten concept of the 'parachor' as a molecular descriptor with respect to the additivity of physical properties in chemical systems dealing specifically with quantitative structure property-activity relationships (QSPR/QSAR).

Introduction

Mechanically interlocked molecules (MIMs)[1] have a rich evolutionary history, encompassing single-station rotaxanes and catenanes,[2] degenerate molecular shuttles,[3] and ultimately bistable molecular switches.[4] The potential for molecular electronics,[5] and other applications,[6] where these molecules have been incorporated and can be addressed by chemical,[7] electrochemical,[8] and photochemical[9] means, is the result of the ability to tune the properties of the molecules themselves through subtle synthetic manipulations. These structural modifications play[10] a key role in the ground-state equilibrium thermodynamics of the molecular switches, which, in turn, carry over to device[5,6] behaviour. Since there are only a few examples of investigations relating to how structural modifications to bistable molecular switches affect their device behaviour, there is a knowledge gap surrounding the consequences of these changes on device properties. Structure–activity investigations, which shed light on this relationship, could lead to more complex MIMs with advanced properties and applications.

The structural parameters that control association constants (K_a) in host–guest[11] complexes can be understood experimentally by comparing the free energy of binding (ΔG°) between different host and guest components. The utility of host–guest binding studies is that they provide a straightforward, thermodynamic understanding of the parameters that affect such binding. An exemplary study by Cram *et al.*,[12] on the binding of primary alkylammonium ion guests in crown ether hosts led to the concepts of preorganisation and complementarity,[13] laying the groundwork for the field of supramolecular chemistry.[11] Herein, we intend to show how similar structure–activity investigations of the binding of donor–acceptor pseudorotaxanes can have an analogous impact on the emerging field of MIMs as switches.

Pseudorotaxanes[14] are supramolecular complexes which consist of a linear guest that is threaded and bound within a macrocyclic host by one or more noncovalent bonding interactions, and this host–guest system is the fundamental, functional precursor that leads, under the guise of templation, to the formation of rotaxanes

[a]*Department of Chemistry, Northwestern University, 2145 Sheridan Road, Evanston, IL 60208-3113, USA). E-mail: stoddart@northwestern.edu; Fax: +1-847-491-1009; Tel: +1-847-491-3793*
[b]*Organic Nanomaterials Center, National Institute for Materials Science, 1-1 Namiki, Tsukuba, 305-0044, Japan*
[c]*School of Chemistry, University of St. Andrews, Purdie Bulding, St. Andrews, Fife, UK KY16 9ST*
[d]*Department of Chemistry and Biochemistry, University of California, Los Angeles, 405 Hilgard Avenue, Los Angeles, CA 90095-1569, USA*
† CCDC reference numbers 720651–720653. For crystallographic data in CIF or other electronic format see DOI: 10.1039/b911874h
‡ These authors contributed equally to this work.

and catenanes.[1–4] In the case of donor–acceptor MIM switches—based on the preferential binding of the cyclobis(paraquat-*p*-phenylene) ($CBPQT^{4+}$) tetracationic cyclophane with the electrochemically active tetrathiafulvalene (TTF) recognition unit over the dioxynaphthalene (DNP) unit[2,4b–i,10]—the difference in the free energy (ΔG^{o}) between these two recognition units can be modelled experimentally by comparing (Fig. 1) the free energy of binding with the diethyleneglycol-disubstituted tetrathiafulvalene (TTF-DEG) and diethyleneglycol-disubstituted 1,5-dihydroxynaphthalene (DNP-DEG) with the host component $CBPQT^{4+}$ during pseudorotaxane formation. Bistable molecular switches, based on these TTF-DEG⊂$CBPQT^{4+}$ and DNP-DEG⊂$CBPQT^{4+}$ binding motifs,[2,4b–i,10] have proven[4–6] to be excellent molecular switches. Switching of these bistable systems can be achieved[10] using either chemical[7] or electrochemical[8] stimuli. The ground-state co-conformation (GSCC), in which the $CBPQT^{4+}$ ring binds preferentially to the TTF recognition unit, is in equilibrium with the metastable-state co-conformation (MSCC), in which the $CBPQT^{4+}$ ring encircles the DNP unit.[10a,c] This equilibrium between the GSCC and the MSCC at 298 K corresponds[10a,c] to a ratio of 9 : 1, or a ΔG^{o} value of about 1.6 kcal mol^{-1}, when the $CBPQT^{4+}$ ring is free to distribute itself between the TTF and DNP recognition units. Calculating the ΔG^{o} of bistable systems from the $\Delta\Delta G^{o}$ of the supramolecular host–guest behavior, we find that $\Delta G^{o}_{GSCC/MSCC} \approx (\Delta G^{o}_{DNP\text{-}DEG\subset CBPQT} - \Delta G^{o}_{TTF\text{-}DEG\subset CBPQT})$ is roughly 1.6 kcal mol^{-1}. The experimentally determined ΔG^{o} for the bistable [2]catenane that uses the same recognition motifs is 1.5 (± 0.2) kcal mol^{-1}, which is in very good agreement with the value predicted by this simple quantitative relation. The pseudorotaxanes form[15] as a result of [π ··· π], [C–H ··· π], and [C–H ··· O] interactions between the π-electron deficient host $CBPQT^{4+}$ and π-electron rich guests, (TTF-DEG) or (DNP-DEG). Structural modifications[16] to either of the recognition units, and/or the cyclophane affects the K_a of complexation, rendering it possible to tune, alter and predict the thermodynamic equilibria of the resulting MIM switches, and consequently, molecular switch-based device performance.

Bistable, donor-acceptor MIMs[4] are usually the end product of a multistep synthesis and, as a result, are rarely carried on to further chemical transformations. While modifications[16] to the guest components are well known, few examples[17] of modifications to the $CBPQT^{4+}$ skeleton exist. A straightforward approach to structural modifications of bistable [2]catenanes, and also bistable [2]rotaxanes, which will permit further transformations, is the functionalisation of the $CBPQT^{4+}$ ring, at a single *ortho* position on one of the *p*-xylyl rings. This strategy has been exploited successfully for attaching molecular switches to surfaces and onto gold nanoparticles through the covalent modification of the $CBPQT^{4+}$ ring, as opposed to the dumbbell, and has resulted in a linear artificial molecular muscle[17a] and nanoparticulated switches.[17b] Since the extent to which covalent modification of the $CBPQT^{4+}$ ring affects guest binding, and thus switching in MIMs has not been studied to any great extent, such an investigation would help to answer the following questions: (1) do the steric effects of appending bulky substituents onto the host alter the binding of guests, and (2) what is the potential for new supramolecular/molecular systems which benefit from these functionalised $CBPQT^{+4}$ rings? It is cumbersome and impractical, however, to synthesise the series of MIMs required to answer these questions. A more rational approach is to study the binding of the individual components as pseudorotaxanes and subsequently extrapolate to the properties of the potential MIMs.

The research reported herein describes a systematic approach to designing and tuning switchable MIMs and MIM-based materials by looking initially at the interactions present in their precursor pseudorotaxanes. This approach bridges the knowledge gap between the binding of supramolecular systems[11,13] and the switchable, mechanically bound[4] molecules. We (1) describe the use of a library of $CBPQT^{4+}$-based hosts in order to understand the effects of substituents on pseudorotaxane formation with a variety of guests using isothermal titration microcalorimetry (ITC) and electrochemistry. The $\Delta\Delta G^{o}$ values between different host–guest complexes can subsequently be extrapolated to predict the switching thermodynamics of analogous MIM switches, employing the same donor–acceptor recognition components. Concurrently, we (2) look to X-ray crystallographic data to illuminate in detail the relationship between supermolecules, *i.e.*, the pseudorotaxanes, and MIMs. Finally, we (3) investigate experimentally the ground-state equilibrium thermodynamics of bistable molecular switches appended to a polymer side-chain by a structurally modified $CBPQT^{4+}$ ring to validate this predictive thermodynamic approach to designing MIM switches in a sterically demanding environment.

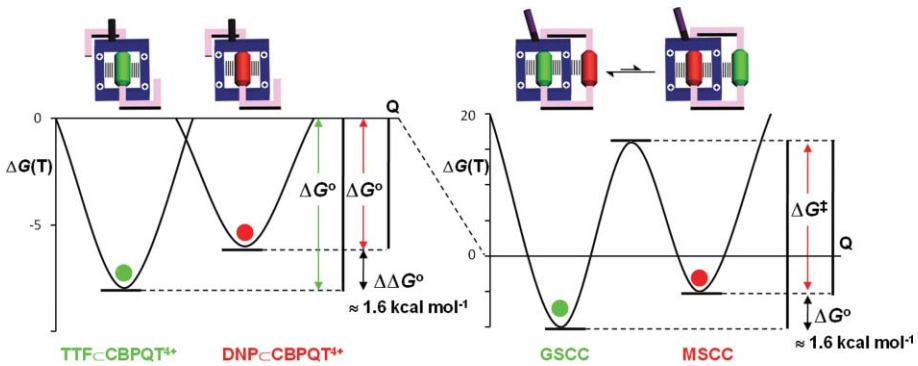

Fig. 1 A comparison of the potential-energy surfaces illustrating (i) two independent host–guest pseudorotaxanes in which the free-energy difference $\Delta\Delta G^{o}$ for TTF⊂$CBPQT^{4+}$ and DNP⊂$CBPQT^{4+}$ correspond to (ii) the ΔG^{o} for GSCC and MSCC in the bistable [2]catenane incorporating the same recognition units, and is defined against a normal coordinate Q, representing circumrotation from the GSCC to the MSCC.

Results and discussion

Structural modification of the host component

The syntheses of 1,4-bis(bromomethyl)-benzene containing OMe, **13**,[18] CO_2H, **14**,[19] CO_2Et, **11**[19] and Br, **12**[20] substituents were carried out as previously described in the literature. The synthesis of the dibromides is shown in Scheme 1. The phenyl-substituted *p*-xylene derivative **8** was synthesised by a Suzuki coupling between phenyl boronic acid and 2,5-dimethylbromobenzene as reported previously.[21] The 1,4-bis(bromomethyl)benzene derivative **10** is of particular significance because it is an example of appending a functional group, a phenyl ring, using a Pd-catalysed coupling to a bromine-functionalised 1,4-bis(bromomethyl)benzene derivative and, eventually, onto the $CBPQT^{4+}$ periphery, a strategy which has the potential to enable the attachment of many functional groups with direct conjugation into the aryl ring of the cyclophane. Dibromides **9** and **10** were prepared by radical bromination of the appropriate *ortho*-substituted 1,4-dimethyl benzene. The substituted 1,4-dimethyl benzenes were mixed with *N*-bromosuccinimide (NBS) and 2,2′-azobis(2-methylpropionitrile) (AIBN) in CH_2Cl_2 and kept under a sodium lamp for 1 day. After the resulting red solution had been filtered to remove the white succinimide precipitate and concentrated *in vacuo*, the resulting orange solid was recrystallised twice in cyclohexane. The dibromide **9** could not be isolated as a pure compound, but its presence in the mixture was confirmed by mass spectrometry. The syntheses of the substituted tetracationic cyclophane hosts **1**–**7**·$4PF_6$ are also shown in Scheme 1. Hosts **6**·$4PF_6$,[19] and **7**·$4PF_6$[25i] were synthesised as previously reported. Generally, the cyclophanes were prepared by mixing the 1,4-bis(bromomethyl) derivatives with **1**·$2PF_6$ in the presence of an excess of DNP-DEG **17** (3 equiv.) in DMF at high-pressure (10–15 kbars).

An azide-functionalised side-chain polymethacrylate[22] was synthesised *via* atom transfer radical polymerisation (ATRP)[22] (Scheme 2). Starting with 2-(2-(2-azidoethoxy)-ethoxy)ethanol **18**, esterification with methacryloyl chloride gave the azide

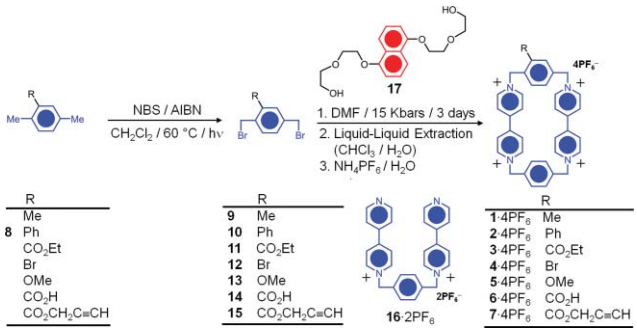

Scheme 1 Template-directed syntheses of the $CBPQT^{4+}$-based host library, in which $CBPQT^{4+}$ has been functionalised at the single *ortho* position on one of the *p*-xylyl rings (R).

monomer **19** in 80% yield. ATRP of monomer **19** using ethyl-2-bromoisobutyrate as the initiator and 4,4′-di(*tert*-butyl)-2,2′-bipyridine as the ligand, with CuBr in Me_2CO gave the desired polymer **20** in 68% yield. It is worth noting at this point that compound **7**·$4PF_6$ does not survive the polymerisation conditions, necessitating post-polymerisation modification of the polymer backbone. Size exclusion chromatography (SEC) analysis of **20** showed a monomodal peak with a $M_w = 55\,000$ g mol^{-1} and $M_n =$ 39,000 g mol^{-1}, PDI = 1.4.

With the aid of autocatalysis,[23] promoted in part by anchimeric assistance[22] during polytriazole formation, polymer **20** was taken to 100% coverage with the alkyne-derivatised $CBPQT^{4+}$ **7**·$4PF_6$ in DMF-d_7 at 60 °C, in the presence of stoichiometric amounts of CuI with an NMR tube serving as the reaction vessel (Scheme 2). The reaction progress was monitored by ^{1}H NMR spectroscopy (Fig. 2a–c). The signals in the ^{1}H NMR spectrum of **21**·$n$$PF_6$ begin to broaden at the onset of the click reaction (Fig. 2b) and are significantly broadened after 3 h (Fig. 2c). The disappearance of the propargyl proton ($-CO_2CH_2C{\equiv}C\mathbf{H}$, δ = 3.75 ppm) of unreacted **7**·$4PF_6$ can be observed with the simultaneous appearance of a broad singlet (δ = 8.55 ppm) for the triazole proton. Additionally, the chemical shift of the propargyl methylene

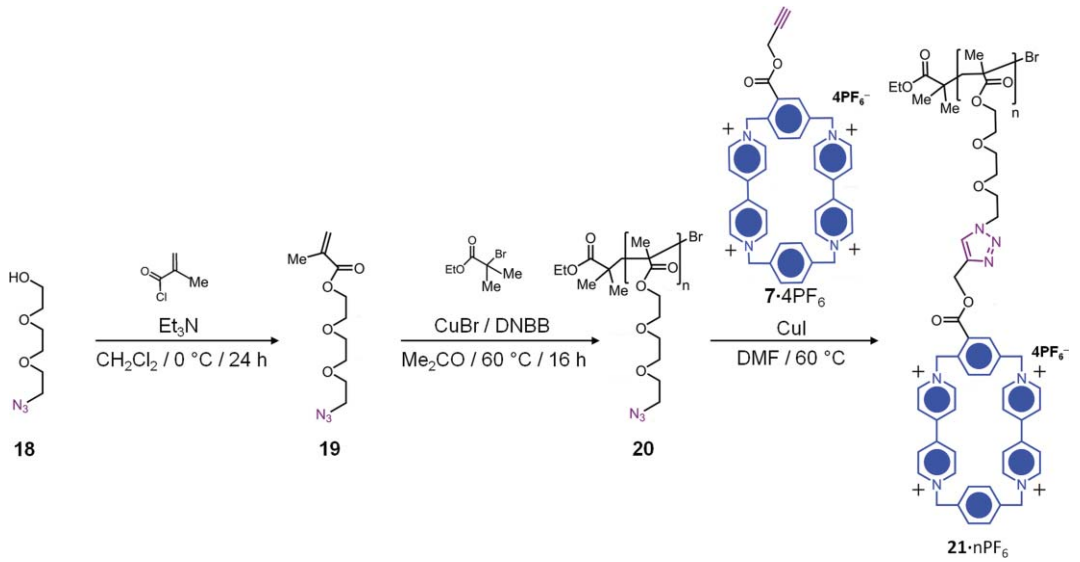

Scheme 2 Synthesis of the side-chain azide-functionalised methacrylate polymer followed by the click functionalisation of azide polymer **20** ($n \approx 160$) with the alkyne-functionalised $CBPQT^{4+}$ derivative **7**·$4PF_6$ for the formation of the side-chain poly$CBPQT^{4+}$ **21**·$n$$PF_6$ ($n \approx 160$).

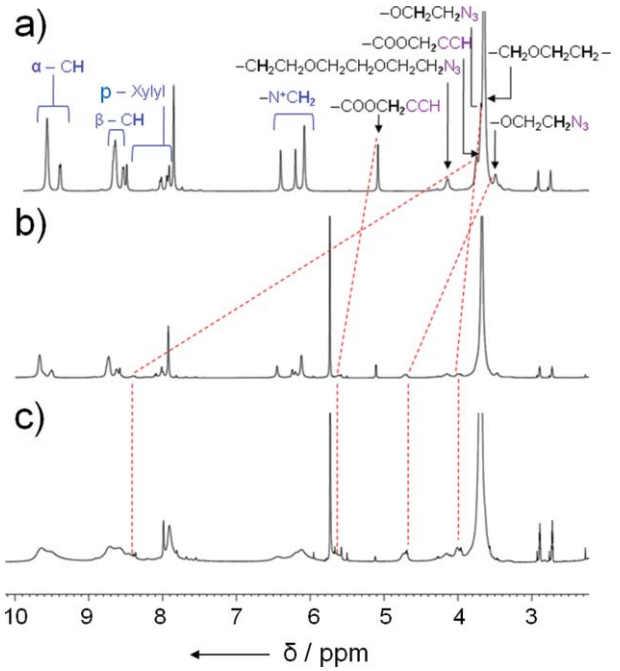

Fig. 2 Stacked ^{1}H NMR spectra recorded in DMF-d_7 at 298 K following the click reaction for the formation of **21**·nPF$_6$ at (a) time = 0, (b) time = 1 h, and (c) time = 3 h.

protons (–CO_2CH_2C≡CH, $\delta = 5.15$ ppm) of unreacted **7**·4PF$_6$ can also be observed at $\delta = 5.6$ ppm in **21**·nPF$_6$ for the –CO_2CH_2–triazole–protons. The protons in the bismethylene unit in the oligoethylene chain closest to the azide function (–$OCH_2CH_2N_3$, $\delta = 3.45$ ppm and –$OCH_2CH_2N_3$, $\delta = 3.69$ ppm) can also be observed to have undergone (–OCH_2CH_2–triazole–, $\delta = 4.70$ ppm; –OCH_2CH_2–triazole–, $\delta = 4.00$ ppm) sizable downfield shifts upon triazole formation. Both the broadening of the peaks for the protons and their chemical shifts in unreacted **7**·4PF$_6$, and of the polymer **20** protons, indicate complete conversion after 3 h, with no further spectroscopic changes being evident after 24 h. Analysis by SEC, coupled with detection by multi-angle light scattering (SEC-MALS)[24] of **21**·nPF$_6$ leads to an M_w of $(9.30 \pm 0.19) \times 10^5$ g mol^{-1}, an M_n value of $(6.10 \pm 0.30) \times 10^5$ g mol^{-1}, and a PDI of 1.5 ± 0.1. Assuming the click reaction[25] proceeds to complete conversion and, based on the molar ratio of the azide functions to the alkyne-functionalised cyclophane **7**·4PF$_6$, a theoretical M_n of 300,000 g mol^{-1} for **21**·nPF$_6$ was calculated, a value which agrees with that estimated from end-group analysis by ^{1}H NMR spectroscopy.

Predicting the thermodynamics of mechanical switching

The ability to derive the thermodynamics of switching in MIMs from the thermodynamic binding properties of the components is a valuable tool that enables the rational design of donor–acceptor bistable [2]catenanes. Experimentally, predicting ΔG° for MIMs is best achieved[10c] by studying the difference in the binding energies ($\Delta\Delta G^\circ$) between the guest components—TTF-DEG and DNP-DEG—with the host component CBPQT^{4+}. The thermodynamic parameters (K_a, ΔG°, ΔH°, ΔS°) determined by ITC,[26] for a library of CBPQT^{4+} derivatives (Scheme 3) that have been structurally modified at a single *ortho* position on one of the *p*-xylyl rings reveals (Table 1) the steric and electronic effects of the substitution (R), compared with CBPQT^{4+} itself (R = H). For all the hosts substituted, the binding strengths are always the greatest when the guest is TTF-DEG, followed by DNP-DEG, and finally by TTF—a trend that is identical to the trends observed with CBPQT^{4+} itself. With a variety of hosts, the differences in the ΔG° values of complexes with TTF varied by no more than 0.5 kcal mol^{-1}. However, the range of ΔG° values increased to approximately 1 kcal mol^{-1} when diethylene glycol chains are appended to the guests. Structural modifications to the host cyclophane decreases the association constant for the formation of the corresponding pseudorotaxane, with the bulky phenyl substituent causing the largest decrease in binding. For the substituents (R), the electron-withdrawing (donating) ability—quantified by the Hammet constant,[27] σ—is an indicator of how the oxidation potential of $TTF^0 \rightarrow TTF^{\bullet+}$ shifts

Table 1 Thermodynamic binding data[a] corresponding to the complexation between the CBPQT^{4+} derivatives and TTF, TTF-DEG, and DNP-DEG guests in MeCN determined by isothermal titration microcalorimetry at 298 K

	CBPQT^{4+}[b]	**1**·4PF$_6$	**2**·4PF$_6$	**3**·4PF$_6$	**4**·4PF$_6$	**7**·4PF$_6$	**22**·nPF$_6$
TTF							
$K_a/\times 10^3$ M^{-1}	6.91 ± 0.18	3.80 ± 1.12	2.19 ± 0.68	3.47 ± 0.07	4.99 ± 0.09	—	—
ΔH°/kcal mol^{-1}	−10.6 ± 0.1	−11.6 ± 1.1	−7.57 ± 0.23	−10.5 ± 0.2	−9.64 ± 0.31	—	—
$T\Delta S^\circ$/kcal mol^{-1}	−5.4 ± 0.1	−6.6 ± 1.1	−2.6 ± 0.1	−5.7 ± 0.2	−4.6 ± 0.3	—	—
$\Delta G^\circ_{298\,K}$/kcal mol^{-1}	−5.27 ± 0.03	−4.91 ± 0.05	−4.94 ± 0.13	−4.79 ± 0.06	−5.07 ± 0.01	—	—
TTF-DEG							
$K_a/\times 10^3$ M^{-1}	380 ± 22.0	212.7 ± 0.9	160.5 ± 8.1	217.5 ± 3.5	348.0 ± 21.0	114.7 ± 1.1	55.4 ± 4.7
ΔH°/kcal mol^{-1}	−14.2 ± 0.1	−13.6 ± 0.9	−12.1 ± 0.1	−14.1 ± 0.1	−13.4 ± 0.4	−11.4 ± 0.1	−9.66 ± 0.22
$T\Delta S^\circ$/kcal mol^{-1}	−6.6 ± 0.1	−6.3 ± 1.0	−5.0 ± 0.2	−6.8 ± 0.1	−5.8 ± 0.5	−4.5 ± 0.1	−3.2 ± 0.3
$\Delta G^\circ_{298\,K}$/kcal mol^{-1}	−7.66 ± 0.07	−7.23 ± 0.27	−7.09 ± 0.05	−7.29 ± 0.01	−7.57 ± 0.02	−6.92 ± 0.05	−6.49 ± 0.05
DNP-DEG							
$K_a/\times 10^3$ M^{-1}	36.4 ± 0.3	13.1 ± 2.2	2.19 ± 0.1	12.9 ± 0.4	17.0 ± 4.2	13.4 ± 1.9	8.02 ± 0.8
ΔH°/kcal mol^{-1}	−15.4 ± 0.1	−15.3 ± 0.7	−12.9 ± 0.6	−14.5 ± 0.1	−14.1 ± 0.2	−13.9 ± 0.6	−14.2 ± 1.5
$T\Delta S^\circ$/kcal mol^{-1}	−9.1 ± 0.1	−9.7 ± 0.8	−8.4 ± 0.7	−8.9 ± 0.1	−8.3 ± 0.2	−8.3 ± 0.5	−8.9 ± 1.5
$\Delta G^\circ_{298\,K}$/kcal mol^{-1}	−6.26 ± 0.04	−5.62 ± 0.09	−4.57 ± 0.02	−5.61 ± 0.04	−5.79 ± 0.02	−5.65 ± 0.07	−5.33 ± 0.05

[a] A 0.39 mM standard solution for all CBPQT^{4+} derivatives was used for all titrations into which solutions of various concentrations of guest were added in 5 mL aliquots (4.7 mM TTF, 3.2 mM TTF-DEG; 3.9 mM DNP-DEG). Hosts **5**·4PF$_6$ and **6**·4PF$_6$ were not measured because of low yield and low binding respectively. Fits were performed using Microcal LLC software. The stoichiometry of all complexes was between 0.99 and 1.02 indicating a 1 : 1 complex is formed. [b] Binding data on CBPQT^{4+} where R = H was obtained from previously published results.[10c]

Table 2 Linear free energy relationships (LFERs): A comparison of the electronic (Hammett Constants (σ_{meta})) and steric (Winstein–Holness *A* values; steric taft parameters (E_s)) contributions to the binding strength (K_a) of TTF-DEG with $CBPQT^{4+}$ for a variety of substituents (R) appended onto the $CBPQT^{4+}$ ring

Host	R	σ [27]	$E_{1/2}$/V[a]	$K_a/\times 10^3$ M^{-1}	*A* value/kcal mol^{-1} [28]	E_s[b]
CBPQT·4PF_6	H	0.00	0.36	380.0 ± 22.0	0.00	1.24
1·4PF_6	Me	–0.07	0.34	212.7 ± 0.9	1.74	0.00
2·4PF_6	Ph	0.06	0.39	160.5 ± 8.1	2.80	–2.55
3·4PF_6	CO_2Et	0.36	0.41	217.5 ± 3.5	1.15	—
4·4PF_6	Br	0.37	0.40	348.0 ± 21.0	0.48–0.67	0.01

[a] The first oxidation potentials of TTF⊃$CBPQT^{4+}$ derivatives were obtained from a 0.4 mM solution of hosts and a 5 mM solution of TTF samples dissolved in MeCN (0.1 M $TBAPF_6$) using a glassy carbon working electrode and a Ag/AgCl reference electrode. [b] Taft parameters for R = CO_2Et have not been reported.

as a result of changes to the electronic structure of the substituted $CBPQT^{4+}$. Table 2 lists the oxidation potential of $TTF^0 \rightarrow TTF^{\bullet+}$ as TTF resides within the cavity of $CBPQT^{4+}$ along with the σ value of the substituent. The host with the substituent that is the least electron-withdrawing, Me ($\sigma = -0.07$) has the lowest measured potential for the oxidation of TTF, and as the electron-withdrawing ability of the substituent increases, so too does the first oxidation potential of TTF^0 in the [2]pseudorotaxane. The cyclophanes with the most electron-withdrawing substituents—**3**·4PF_6 ($\sigma = 0.36$) and **4**·4PF_6 ($\sigma = 0.37$)—cause the $TTF^0 \rightarrow TTF^{\bullet+}$ oxidation potential to shift anodically compared to $CBPQT^{4+}$ derivatives with less electron-withdrawing substituents. This study demonstrates that small changes to the $CBPQT^{4+}$ constitution alters the first oxidation potential of TTF^0 by up to 60 mV as a result of changes in electronic structure that occur from adding a single substituent to the $CBPQT^{4+}$ skeleton. A linear relationship, however, cannot be discerned from a Hammett plot constructed from known Hammett constants (σ) and the experimentally determined binding constants (K_a), since pseudorotaxane formation is not solely governed by electronic effects, but can also be influenced by steric interactions between the substituent and the guests. Linear free energy relationships (LFERs) describing steric size for each substituent (R)—quantified by both the Winstein–Holness *A* values,[28] and steric Taft parameters[29] (E_s)—suggests (Table 2) that pseudorotaxane formation is strongly perturbed as a function of steric hindrance. Previous investigations have highlighted[15] the importance of [C–H···O] interactions during pseudorotaxane formation between the oligoethyleneglycol oxygen atoms and the methylene hydrogen atoms in $CBPQT^{4+}$ in establishing a strong association constant with guests TTF-DEG and DNP-DEG. The solid-state crystal superstructure (Fig. 3b) of DNP-DEG⊂$\mathbf{1}^{4+}$ reveals that the source of the weaker binding is a result of the loss of a [C–H···O] interaction since the glycol chain is disrupted to avoid unfavourable steric interactions with the R group, whereas the oligoethylene glycol chains wrap[1] the $CBPQT^{4+}$ ring at the methylene positions. Indeed we find that **1**·4PF_6 experiences weaker binding interactions (Table 1) with TTF-DEG (212.7 ± 0.97) × 10^3 M^{-1} and DNP-DEG (13.1 ± 2.20) × 10^3 M^{-1} compared to that of $CBPQT^{4+}$ (380.0 ± 22.0) × 10^3 M^{-1} and (36.4 ± 0.25) × 10^3 M^{-1}, respectively.[10c]

The thermodynamic parameters[26] obtained by ITC during pseudorotaxane formation are listed in Table 1 for each of the $CBPQT^{4+}$ derivatives. The difference in the free energies of binding ($\Delta\Delta G^o$) between TTF-DEG *versus* DNP-DEG have been shown to correlate[10a,c] directly to the ΔG^o values for the GSCC *versus* MSCC for the corresponding mechanically interlocked bistable switch, such that $\Delta\Delta G^o \approx \Delta G^o_{predicted}$. The binding data indicate that substitution at the *ortho* position of one *p*-xylylene ring disrupts the [C–H···O] interaction, reducing binding. However, for bistable MIMs, this reduction in binding strength does not result in a change in $\Delta\Delta G^o$ because binding with TTF-DEG and DNP-DEG are reduced equally. Scheme 4 illustrates the thermodynamic equilibrium between the GSCC and the MSCC for bistable [2]catenanes that have been structurally modified

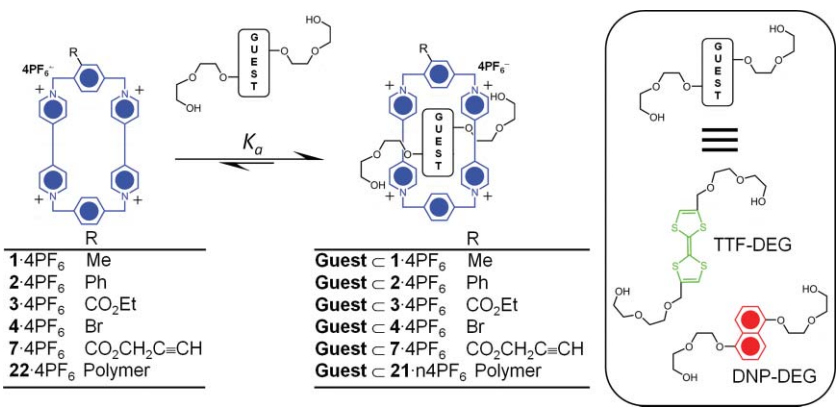

Scheme 3 Pseudorotaxane formation between the $CBPQT^{4+}$ hosts and the diethyleneglycol-disubstituted tetrathiafulvalene (TTF-DEG) and diethyleneglycol-disubstituted 1,5-dihydroxynaphthalene (DNP-DEG).

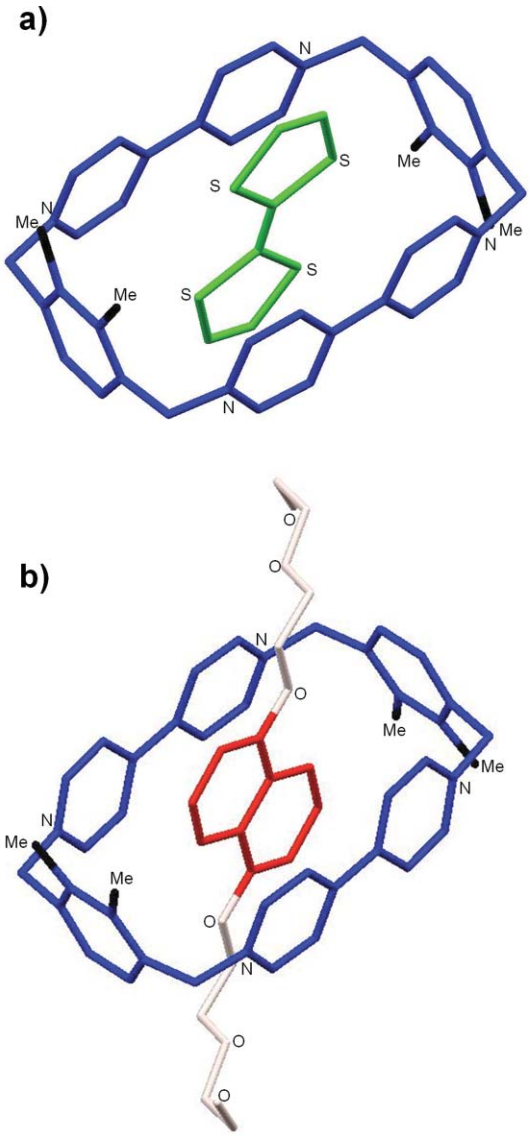

Fig. 3 Stick representations of the solid-state superstructures of (a) TTF⊂$\mathbf{1}^{4+}$ and (b) DNP-DEG⊂$\mathbf{1}^{4+}$ pseudorotaxanes. Additional methyl groups attached to $\mathbf{1}^{4+}$ reflect disorder in the crystal.

at the *ortho* position of the *p*-xylylene unit, and the predicted ΔG^{o} values for the structures. These $\Delta G^{o}_{predicted}$ values for the bistable [2]catenanes agree well with the free energy profiles for molecular motions in bistable molecules obtained by Goddard *et al.*[30] using molecular dynamic simulations, and from previous experiments[10a,c] using bistable [2]rotaxanes in a variable temperature cyclic voltammetry study. These predicted results demonstrate that modification at the *ortho* position of $CBPQT^{4+}$ should not perturb significantly the switching behaviour, suggesting that molecular switches with *ortho*-substituted $CBPQT^{4+}$ rings are indeed candidates for future device applications. To what extent these predictions correlate with the actual experimental values for ΔG^{o} in bistable [2]catenanes must now be considered. To validate directly these predictions on a bistable [2]catenane, the alkyne-functionalised dibromide precursor **15** was used to synthesise the corresponding alkyne-derivatised bistable [2]catenane **23**·4PF_6 in order to study its switching behaviour as a small molecule [2]catenane. Further support for the thermodynamic relationship between the pseudorotaxanes and catenanes following the formation of the mechanical bond was obtained[31] by synthesising a side-chain poly[2]catenane using the alkyne-derivatised bistable [2]catenane **23**·4PF_6 precursor, and studying its ground state equilibrium and thermodynamic properties.

Structural modification of the bistable [2]catenane

In order to form **23**·4PF_6 by way of template-directed synthesis[32] (Scheme 5), **16**·2PF_6 was added to a solution of the dibromide **15** and macrocycle **22** in dry DMF. The reaction mixture was stirred for a week. The ^{1}H–^{1}H g-DQF-COSY (Fig. 4b) of **23**·4PF_6 in CD_3CN at 298 K reveals correlation peaks between the α and β protons of the $CBPQT^{4+}$ ring. The peaks for the protons H-3/7 and H-4/8 of the DNP recognition unit are hidden underneath the signals for the *p*-xylylene protons of the $CBPQT^{4+}$ ring in the ^{1}H NMR spectrum (Fig. 4a). The COSY spectrum (Fig. 4b) shows clearly the correlation peaks for the overlapping H-3/7 and H-4/8 protons of DNP. Correlations between the propargyl methylene protons and the unreacted alkyne proton can also be observed. Correlations among the glycol chain protons can be detected but are not well-resolved.

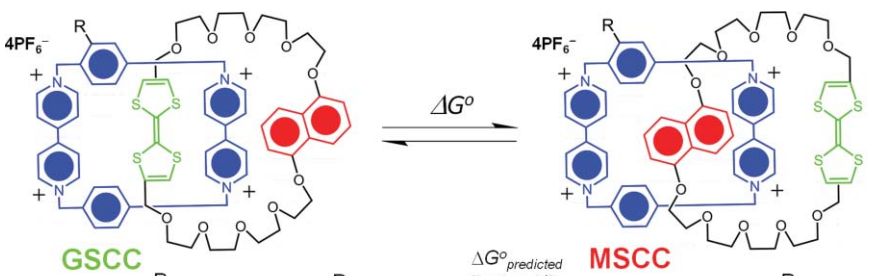

GSCC	R
GSCC1·4PF_6	Me
GSCC2·4PF_6	Ph
GSCC 3·4PF_6	CO_2Et
GSCC 4·4PF_6	Br
GSCC 7·4PF_6	$CO_2CH_2C{\equiv}CH$
GSCC 24·nPF_6	Polymer

R	$\Delta G^{o}_{predicted}$ [kcal mol^{-1}]
Me	1.61 (± 0.29)
Ph	2.53 (± 0.05)
CO_2Et	1.68 (± 0.02)
Br	1.78 (± 0.03)
$CO_2CH_2C{\equiv}CH$	1.28 (± 0.09)
Polymer	1.16 (± 0.07)

MSCC	R
MSCC1·4PF_6	Me
MSCC2·4PF_6	Ph
MSCC 3·4PF_6	CO_2Et
MSCC 4·4PF_6	Br
MSCC 7·4PF_6	$CO_2CH_2C{\equiv}CH$
MSCC 24·nPF_6	Polymer

Scheme 4 Translating the thermodynamics from supramolecular host–guest behaviour ($\Delta\Delta G^{o}$) to predicted free energy of binding ($\Delta G^{o}_{predicted}$) for an interlocked bistable catenane library, where the host $CBPQT^{4+}$ has been functionalised at the single *ortho* position on one of the *p*-xylyl rings (R).

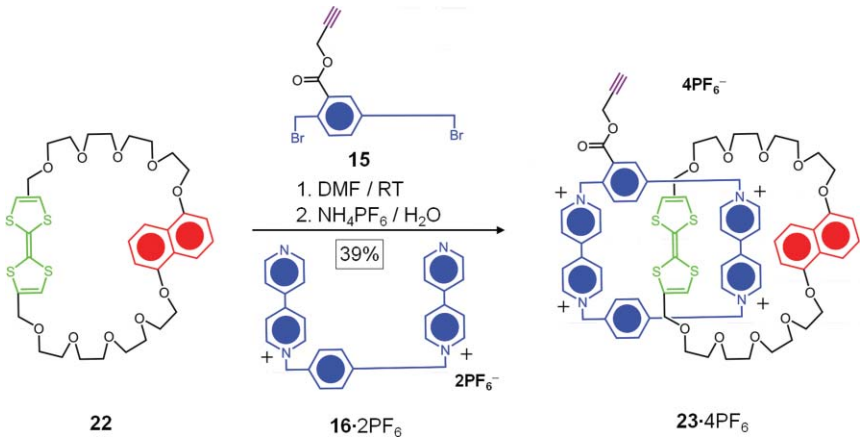

Scheme 5 Template-directed synthesis of the alkyne-functionalised bistable [2]catenane.

Slow vapour diffusion of *i*-Pr_2O into a MeCN solution of **23**·4PF_6 afforded green crystals suitable for X-ray analysis (Fig. 5). Of the two configurational isomers, only the "*trans*" isomer of the disubstituted TTF on the two-station crown ether macrocycle is observed[4b] in the solid-state structure of **23**·4PF_6. The alkyne-functionalised [2]catenane is stabilised by the same [π···π], [C–H···π] and [C–H···O] interactions that are also present[1a] in the psuedorotaxane model complexes. In fact, a closer examination of the solid-state crystal superstructure of pseudorotaxanes DNP-DEG⊂**1**·4PF_6 and TTF⊂**1**·4PF_6 (Fig. 6a–b) reveals that the guests adopt[1a] the same co-conformation within the host $CBPQT^{4+}$ as the DNP and TTF binding sites within the alkyne-derivatised [2]catenane **23**·4PF_6, including identical values (Table 3) for the [H···O[c]] and [H···O[e]] bond distances, and the [C–H···O[d]] bond angle. The discrepancy in the second [C–H···O[f]] bond angle, however, is a result of the guests residing in a crown ether macrocycle as opposed to the linear thread of the pseudorotaxane. The observed difference in the [π···π[h]] bond distance is a result of the DNP recognition unit no longer residing within the $CBPQT^{4+}$ ring as the guest in the interlocked species. The solid-state crystal structure (Fig. 5) of **23**·4PF_6 also reveals that the source of the weaker binding during pseudorotaxane formation is a result of the loss of a [C–H···O] interaction since the glycol chain is displaced to avoid unfavourable steric interactions with the R group on the host, which results in an unusual kink in the glycol chain of the π-electron rich macrocycle whereas the solid-state crystal structures of similar underivatised bistable [2]catenanes[4b] have no such kink. These observations illustrate the obvious link[1a] between the noncovalent bonding interactions in pseudorotaxanes and MIMs that survive following the formation of the mechanical bonds. Furthermore, the solid-state packing of **23**·4PF_6 (Fig. 7) is comprised of intermolecular donor–acceptor [π···π] interactions between the outside electron-deficient bipyridinium units and the alongside electron rich DNP units of adjacent [2]catenanes. These

Table 3 Comparison of the crystallographic parameters of the solid-state superstructures for the pseudorotaxanes DNP-DEG⊂**1**·PF_6, TTF⊂**1**·PF_6 and bistable [2]catenane **23**·4PF_6

	DNP-DEG⊂**1**·4PF_6[a]	TTF⊂**1**·4PF_6[a]	**23**·4PF_6[b]
Formula	$C_{67}H_{67}N_{10}O_6(4PF_6)$	$C_{43}H_{38}N_4S_4(4PF_6)$	$C_{74}H_{78}N_4O_{12}S_4{\cdot}6.5H_2O{\cdot}C_6H_{14}O(4PF_6)$
Mass	1697.26	1392.79	2142.80
Space group	$P2_1/n$	$P2_1/n$	$P2_1/c$
Symmetry	C_i	C_i	—
a/Å	13.83834 (9)	10.8498 (8)	14.216 (4)
b/Å	23.2237 (16)	19.3989 (14)	54.971 (12)
c/Å	13.0531 (9)	13.8729 (10)	13.678 (4)
[H···O][c]/Å	2.38	—	2.33
[C–H···O][d]/°	152	—	156
[H···O][e]/Å	2.46	—	2.35
[C–H···O][f]/°	142	—	175
[C–H···π][g]/Å	2.57	—	—
[π···π][h]/Å	3.76	—	3.53
[π···π][i]/Å	—	3.80	3.80

[a] See Fig. 3. [b] See Fig. 5. [c] Length refers to the [H···O] interactions between O_3 of the glycol chain of the DNP guest/station and the methylene hydrogen of the host. [d] Angle refers to the [C–H···O] interactions between O_3 of the glycol chain of the DNP guest/station and the methylene hydrogen of the host. [e] Length refers to the [H···O] interactions between O_2 of the glycol chain of the DNP guest/TTF station and the H_α on the bipyridine of the host. [f] Angle refers to the [C–H···O] interactions between O_3 of the glycol chain of the DNP guest/TTF station and the H_α on the bipyridine of the host. [g] Length refers to the [C–H···π] interactions between H_1 of the naphthalene rings of DNP-DEG and the aryl rings of the host. [h] Length refers to the [π···π] interactions between naphthalene rings of DNP-DEG and the aryl rings of the host. [i] Length refers to the [π···π] interactions between TTF guest and the aryl rings of the host.

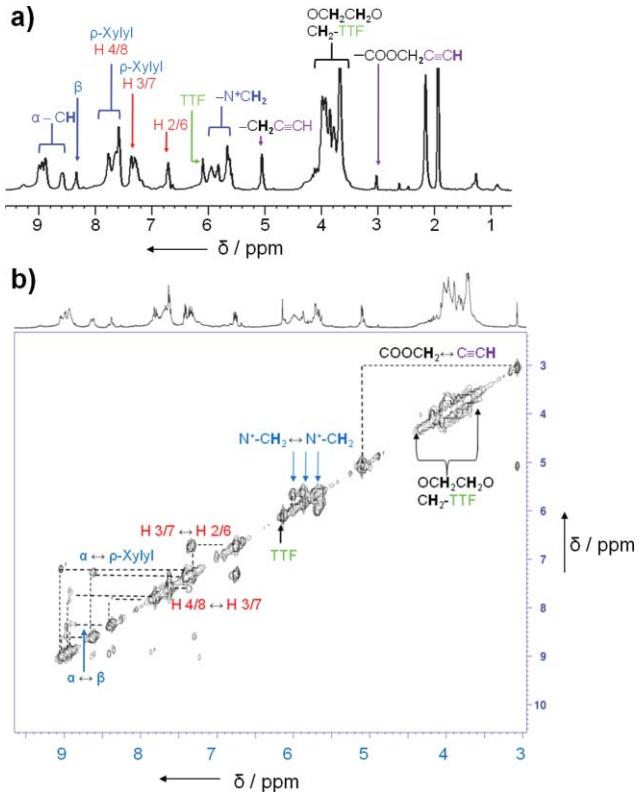

Fig. 4 (a) ^{1}H NMR spectrum of **23**·PF_6 in CD_3CN at 298 K. (b) The ^{1}H–^{1}H g-DQF-COSY spectrum of **23**·PF_6 in CD_3CN at 298 K.

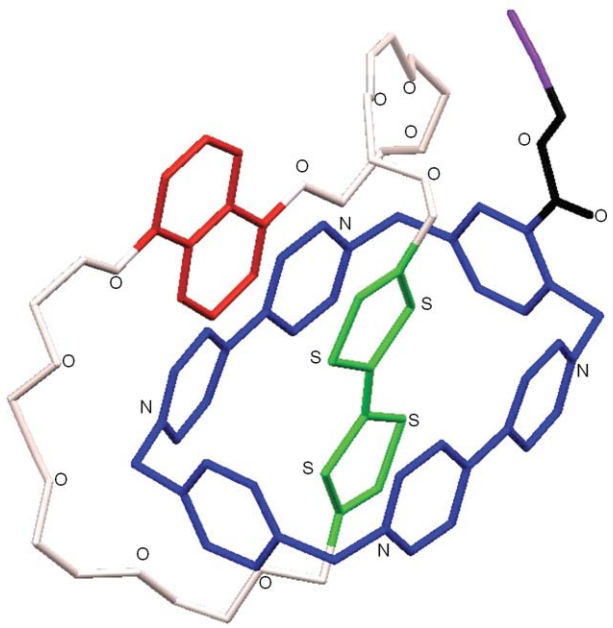

Fig. 5 A stick representation of the solid-state crystal structure of the alkyne-functionalised bistable [2]catenane **23**$^{4+}$.

intermolecular interactions may also contribute to the previously observed[31] aggregation of bistable side-chain poly[2]catenanes in solution, but more importantly they serve as a reminder highlighting the presence of the noncovalent bonding interactions that are present not only in the psuedorotaxanes, but also in MIMs as well.

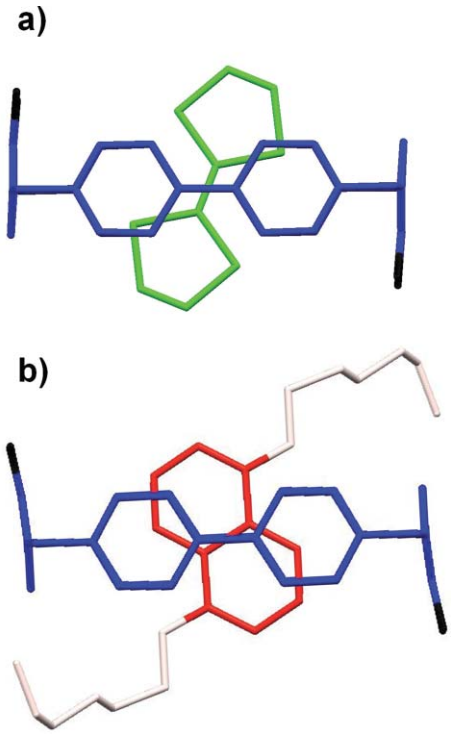

Fig. 6 Side-on views of the solid-state superstructure of (a) TTF⊂**1**$^{4+}$ and (b) DNP-DEG⊂**1**$^{4+}$ pseudorotaxanes showing the co-conformations of host and guests when bound within the CBPQT^{4+} host cavity. Additional methyl groups attached to **1**$^{4+}$ reflect disorder in the crystal.

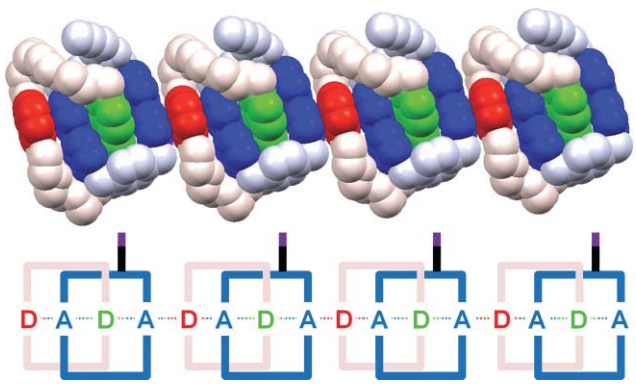

Fig. 7 (a) A space-filling representation of the packing of the alkyne-functionalised bistable [2]catenane **23**$^{4+}$ molecule in the solid-state, illustrating the intermolecular donor–acceptor [$\pi \cdots \pi$] interactions between the DNP recognition unit (red ≡ D) sitting outside the CBPQT^{4+} host which contains a TTF recognition unit (green ≡ D) with the outside Bipy^{2+} unit of the CBPQT^{4+} ring. (b) A graphical representation of the polar stack present in the solid-state of **23**$^{4+}$.

The synthesis (Scheme 6) of the bistable side-chain poly[2]catenane proceeded much like the synthesis of the side-chain polyCBPQT^{4+} **21**·*n*PF_6. Polymer **20** was taken to 27% side-chain modification with the alkyne-derivatised [2]catenane **23**·4PF_6 in DMF-d_7 at 60 °C, in the presence of stoichiometric CuI, again with an NMR tube serving as the reaction vessel. The click reaction progress was monitored by ^{1}H NMR spectroscopy (Fig. 8a–d). The resonances in the ^{1}H NMR spectrum (Fig. 8a) of **24**·*n*PF_6 begin to broaden at the onset of the click reaction, and

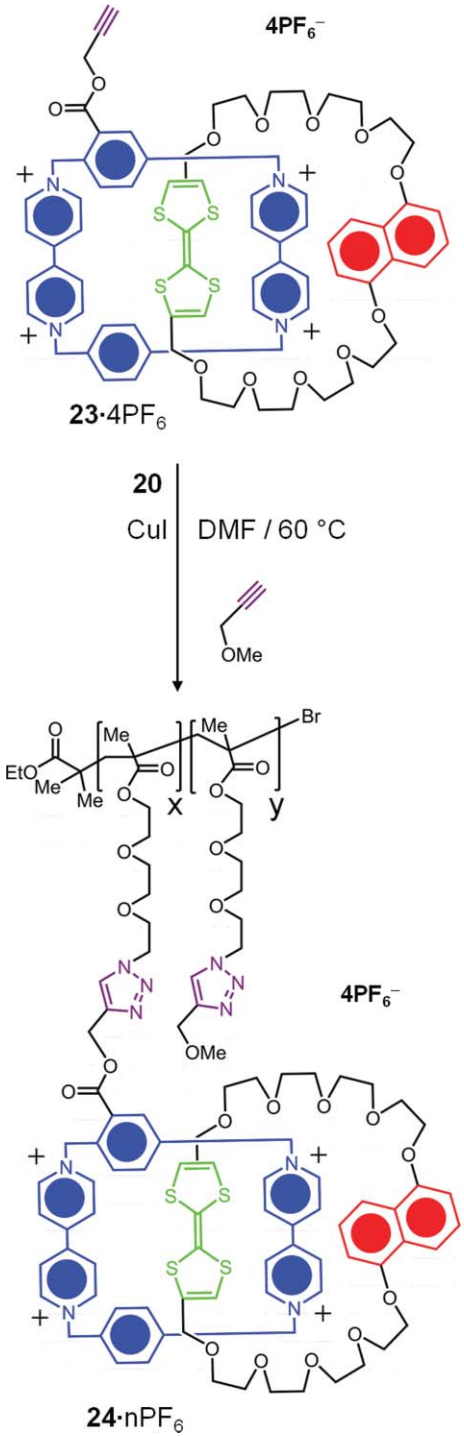

Scheme 6 Click functionalisation of polymer **20** ($n \simeq 160$) with the alkyne-functionalised bistable [2]catenane **23**·4PF_6 for the formation of **24**·$n$$PF_6$ ($x \simeq 42$, $y \simeq 118$).

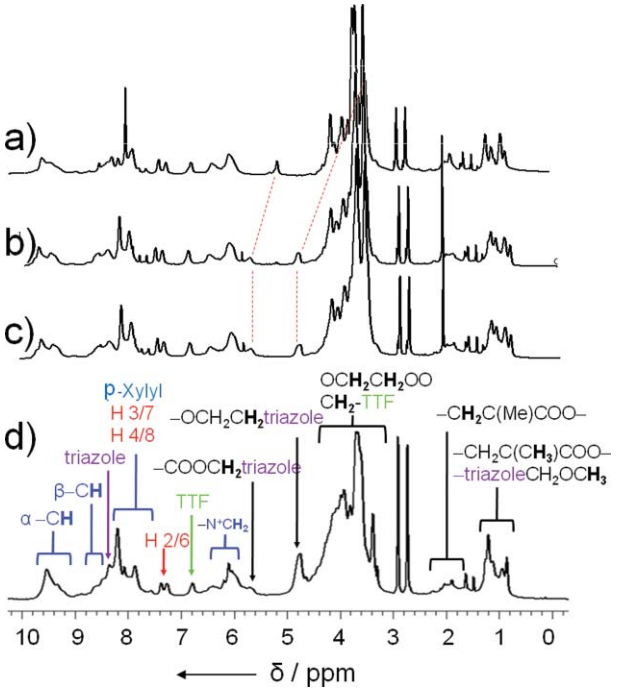

Fig. 8 Stacked ^{1}H NMR spectra in DMF-d_7 at 298 K following the click reaction that leads to the formation of **24**·$n$$PF_6$ at (a) time = 0, (b) time = 1 h, (c) time = 3 h, and (d) after capping the remaining azide moieties with methyl propargyl ether.

are significantly broadened after 3 h. Additionally, the chemical shift of the propargyl methylene protons (–$CO_2CH_2C{\equiv}CH$, δ = 5.15 ppm) in unreacted **23**·4PF_6 can be observed at δ = 5.6 ppm in **24**·$n$$PF_6$ for the –CO_2CH_2–triazole–protons. The signals for the protons in the bismethylene unit in the oligoethylene chain closest to the azide funtion (–$OCH_2CH_2N_3$, δ = 3.45 ppm) can also be observed to have undergone (–OCH_2CH_2–triazole–, δ = 4.70 ppm) sizable downfield shifts upon triazole ring formation. Both the broadening of the peaks for the protons and the chemical shifts of the protons in unreacted **23**·4PF_6, and of the polymer **20** protons indicate complete conversion after 3 h, with no further spectroscopic changes evident after 24 h. Following the functionalisation of **20** with **23**·4PF_6, the unreacted azides can be capped by reacting the product with methyl propargyl ether. This step (Fig. 8d) shows a dramatic increase in the peak areas for the triazole protons (δ = 8.55 ppm), as well as for the side-chain bismethylene protons closest to the azide moiety (–OCH_2CH_2–triazole–, δ = 4.70 ppm), and the appearance of a broad resonance for the methyl protons (–triazole–CH_2OCH_3, δ = 1.19 ppm). Analysis by SEC-MALS[24] of **24**·$n$$PF_6$ produces a M_w value of (1.30 ± 0.07) × 10^6 g mol^{-1}, a M_n value of (8.70 ± 0.61) × 10^5 g mol^{-1}, and a PDI of 1.5 ± 0.1. Assuming the click reaction proceeds to complete conversion and, based on the molar ratio of the azide functions to the alkyne-functionalised cyclophane **7**·4PF_6, a theoretical M_n of 128 000 g mol^{-1} for **24**·$n$$PF_6$ was calculated, a value which agrees with that estimated from end-group analysis by ^{1}H NMR spectroscopy.

Ground state equilibrium thermodynamics

Tetrathiafulvalene can undergo[4b–i,10] a two-electron oxidation process (TTF → $TTF^{\bullet+}$ → TTF^{2+}), generating cationic species, at which point switching through circumrotation in **23**·4PF_6 and **24**·$n$$PF_6$ of the macrocyclic polyether with respect to the $CBPQT^{4+}$ ring occurs. Upon reduction of the cationic species back to the neutral form, the MSCC relaxes to the equilibrium mixture of the GSCC and MSCC.[4b–i,10] Switching of the GSCC to the MSCC can be achieved electrochemically or chemically.

Table 4 Ground-state equilibrium thermodynamic parameters (ΔH°, ΔS°, ΔG°_{298K}) obtained after analysis of variable-temperature UV-vis experiments

Species	$\Delta H^{\circ a}$/kcal mol^{-1}	$T\Delta S^{\circ b}$/kcal mol^{-1}	$\Delta G^\circ_{298K}{}^{c}$/kcal mol^{-1}	$\Delta G^\circ_{predicted}{}^{d}$/kcal mol^{-1}
23·4PF$_6$	3.9 (± 0.1)	2.4 (± 0.2)	1.5 (± 0.2)	1.3 (± 0.1)
24·*n*PF$_6$	3.8 (± 0.1)	2.2 (± 0.1)	1.6 (± 0.1)	1.2 (± 0.1)

[a] Obtained from a linear van't Hoff plot where the slope of the line is equal to $-\Delta H^\circ/R$. [b] Obtained from a linear van't Hoff plot where the the intercept is equal $\Delta S^\circ/R$. [c] Calculated from the Gibbs free energy identity $\Delta G^\circ = \Delta H^\circ - T\Delta S^\circ$. [d] Predicted from the difference in the free energies of binding ($\Delta\Delta G^\circ$) between TTF-DEG *versus* DNP-DEG with hosts **7**·4PF$_6$ and **22**·*n*PF$_6$ obtained by ITC in MeCN at 298 K.

The thermochromic properties of both the **23**·4PF$_6$ and **24**·*n*PF$_6$ were examined (Fig. 10) by variable temperature (VT) UV-vis spectroscopy in DMF in order to quantify the ground-state equilibrium thermodynamic parameters. The CT band situated at 812 nm is characteristic[10b] of the (GSCC), whereas the (MSCC) produces a characteristic[10b] CT band at 475 nm in DMF. Upon cooling the solution, the TTF⊂CBPQT^{4+} CT band (ε = 4000 L mol^{-1} cm^{-1}) increases in intensity, while the DNP⊂CBPQT^{4+} CT band decreases. This observation indicates that the equilibrium between the translational isomers favors the GSCC at lower temperatures. Upon heating, the opposite trend is observed. With the aid of VT ^{1}H NMR spectra (Fig. 9) recorded to determine the equilibrium constant for the GSCC/MSCC ratio in **23**·4PF$_6$ by monitoring the DNP 2/6 proton resonances ($\delta \approx 6.7$ ppm) at 298 K, van't Hoff plots were constructed[33] (Fig. 10a–b inset)

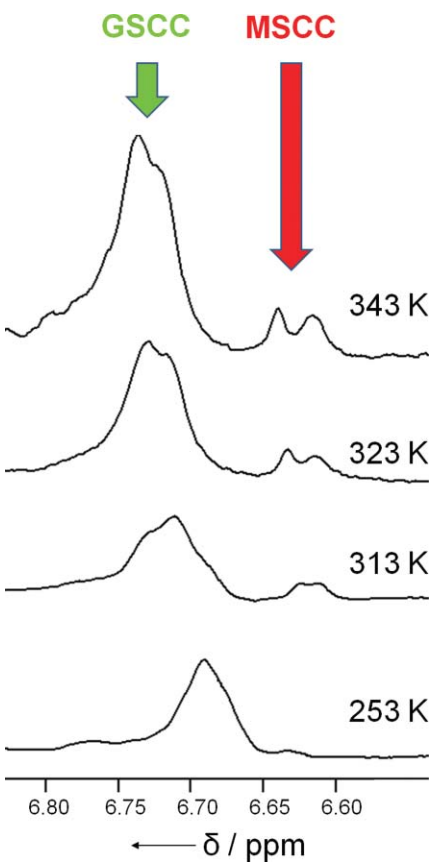

Fig. 9 Partial variable temperature ^{1}H NMR stacked spectra of **23**·4PF$_6$ taken in CD$_3$CN showing the temperature-dependent equilibrium between the GSCC and the MSCC by using the H-2/6 protons of the DNP recognition unit as probe protons.

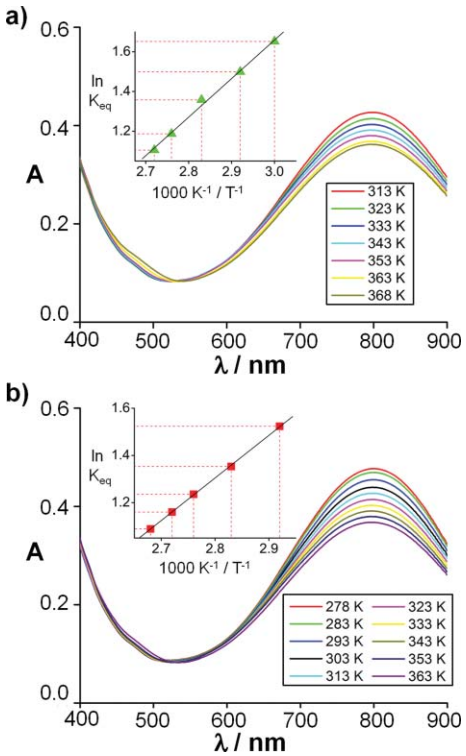

Fig. 10 (a) Variable temperature UV-vis spectra of the alkyne-functionalised [2]catenane **23**·4PF$_6$ and (b) the side-chain poly[2]catenane **24**·*n*PF$_6$ (2×10^{-4}M, DMF), illustrating the temperature-dependent equilibrium between GSCC (TTF⊂CBPQT^{4+} charge transfer band at 800 nm) and MSCC (DNP⊂CBPQT^{4+} charge transfer band at 480 nm). Linear van't Hoff plots for **23**·4PF$_6$ (R^2 = 0.996) and **24**·*n*PF$_6$ (R^2 = 0.996) for the thermally induced GSCC → MSCC equilibrium change was employed to calculate the ΔG°_{298K}, ΔH°, and ΔS° values for the process and are tabulated in the Table 4.

in order to obtain (Table 4) the standard enthalpy (ΔH°) and standard entropy ($T\Delta S^\circ$) changes for the GSCC→MSCC process. The GSCC→MSCC processes in **23**·4PF$_6$ and **24**·*n*PF$_6$ correspond to ΔG° values of 1.5 (± 0.2) and 1.6 (± 0.1) kcal mol^{-1}, respectively. Van't Hoff plots constructed using integration of the resonance peaks from the VT ^{1}H NMR experiment for **23**·4PF$_6$ also leads to a ΔG° value of ≈ 1.6 kcal mol^{-1}. Attempts at VT ^{1}H NMR characterisation of **24**·*n*PF$_6$ to probe switching proved impractical as a consequence of overlapping resonances and characteristic broadening of high molecular weight polymers. The observed ΔG° values for both **23**·4PF$_6$ and **24**·*n*PF$_6$, namely 1.5 (± 0.24) and 1.6 (± 0.05) kcal mol^{-1}, respectively, agree well with the predicted values found (Table 4) by determining the $\Delta\Delta G^\circ$ of

the pseudorotaxane components. Additionally the data in Table 4 also indicate that the GSCC→MSCC switching process for both **23**·4PF_6 and **24**·*n*PF_6 is enthalpy driven as indicated by the larger enthalpic contribution over the entropic contribution (ΔH° = 3.9 (± 0.1) kcal $mol^{-1}_{\mathbf{23}\cdot 4PF_6}$, ΔH° = 3.8 (± 0.1) kcal $mol^{-1}_{\mathbf{24}\cdot n PF_6}$; $T\Delta S^\circ$ = 2.4 (± 0.2) kcal $mol^{-1}_{\mathbf{23}\cdot 4PF_6}$, $T\Delta S^\circ$ = 2.2 (± 0.1) kcal $mol^{-1}_{\mathbf{24}\cdot n PF_6}$). A comparison of the thermodynamic parameters from Table 1 and Table 4, also indicates that pseudorotaxane formation is an enthalpy driven process, having a much larger enthalpic contribution during the threading process than the GSCC→MSCC process in the [2]catenane. This situation can be explained by the inherent differences between a process in which solvent molecules must be displaced from the inside of $CBPQT^{4+}$ ring during pseudorotaxane formation, and circumrotation in the catenated species, which does not require the displacement of solvent molecules or the unraveling of the linear glycol chains of the guest. Despite the inherent differences between the processes of pseudorotaxane formation and circumrotation, thermodynamic compensation ensures that the free energy (ΔG°) for both processes remains closely related.

Conclusions

We have demonstrated that a reliable comparison exists between the thermodynamic free energy differences ($\Delta\Delta G^\circ$) observed for the binding of different guests with modified hosts, and the thermodynamic free energy of switching (ΔG°) of the analogous bistable [2]catenanes made with the same components. A small library of π-electron deficient $CBPQT^{4+}$ hosts, modified at the *ortho* positions on one of the *p*-xylylene rings, was synthesised, and the consequences of the substitutions upon their binding of π-electron rich guests were evaluated by means of ITC studies and X-ray crystallography. A decrease in the binding constants was observed for all guests interacting with the substituted host $CBPQT^{4+}$ ring when compared to the unsubstituted host, $CBPQT^{4+}$, as a result of the loss of a single [C–H · · · O] interaction. This observation was further supported by studying the linear free energy relationships (LFERs) describing steric size for each substituent (R)—quantified by both the Winstein-Holness *A* values,[28] and steric Taft parameters[29] (E_s)—and the influence of such on the binding strength of the host and guest (K_a). However, the behaviour of the resulting bistable catenanes is unchanged because the interactions of the cyclophane with both recognition units are diminished to the same extent. This behaviour was illustrated by synthesising an alkyne-modified bistable [2]catenane, as well as a polymer with a bistable [2]catenane side-chain modification. In both systems, the switching thermodynamics were comparable to the unmodified bistable [2]catenane, and the switching thermodynamics could be predicted by inspection of the $\Delta\Delta G^\circ$ values of the components enabling accurate predictions without cumbersome synthesis. The additivity of the thermodynamic differences ($\Delta\Delta G^\circ$) observed for binding of different guests with modified hosts, and the thermodynamic switching parameters (ΔG°) in MIMs is consistent, at the very least, with the long forgotten concept[34] of the 'parachor', where these thermodynamic quantities, obtained from two separate binding experiments "which are *a priori* independent", require[35] the examination of their influence on the switching behavior of the analogous MIM, and their "eventual statistical dependence *a posteriori*".

Experimental

Materials and methods

All solvents (Fischer Scientific) were dried prior to use. All reagents and starting materials were purchased from Aldrich or VWR and used without further purification. **6**·4PF_6,[19] **7**·4PF_6,[25h] **8**,[18] **11**,[19] **12**,[20] **13**,[18] **14**,[19] **15**,[25h] **16**·2PF_6,[25h] **17**,[25h] **22**[4b] and TTF-DEG[10b] were prepared according to published literature procedures. Thin-layer chromatography was carried out using aluminum sheets precoated with silica gel 60 (Merck 40–60 mm, 230–400 mesh). Melting points are uncorrected. Deuterated solvents (Cambridge Isotope Laboratories) for NMR spectroscopic analyses were used as received. Column chromatography was performed on silica gel 60 (Merck 40–60 nm, 230–400 mesh). Size exclusion chromatography was performed using an Agilent 100 Series pump with a Viscotek ViscoGEL GPC column, coupled to a Wyatt DAWN HELEOS-II multi-angle light scattering detector and an OPTILAB rEX refractive index detector. NMR Spectra were recorded on Varian INOVA-400 (at 400 MHz), Varian INOVA-500 (at 500 MHz), Varian P INOVA-500 (at 500 MHz), and Varian INOVA-600 (at 600 MHz) spectrometers. All chemical shifts are quoted in ppm, relative to tetramethylsilane, using the residual solvent peak as a reference standard. Mass spectra were measured on an IonSpec 7.0T Ultima FTMS with ESI and MALDI ion sources. Electrochemistry was performed using a Gamry Reference 600 potentiostat/galvanostat/ZRA.

General procedure of the cyclisation to form tetracationic cyclophane hosts

1, 1′ - [1 , 4 - Phenylenebis - (methylene)] bis (4 , 4′ - bipyridinium) bis(hexafluorophosphate) (1 equiv.) was added to a solution of the appropriate dibromo-*p*-xylene derivative (1 equiv.) and the template **17** (3 equiv.) dissolved in DMF. The reaction mixture was subjected to high pressure (10–15 kbar) for three days. The solvent was removed from the resulting purple solution under vacuum, and the purple oil was subjected to liquid–liquid extraction [$CHCl_3$/1% (w/v) NH_4Cl (aq)] until the solution became colourless. The solvent was removed from the aqueous portion and the resulting solid was subjected to column chromatography [SiO_2: MeOH/$MeNO_2$/2 M NH_4Cl (7 : 1 : 2)]. The eluent was removed *in vacuo*, the solid was dissolved in hot H_2O and a saturated aqueous solution of NH_4PF_6 was added until no further precipitate was observed. The precipitate was recovered by filtration to give the appropriate tetracationic cyclophane as its tetrakis(hexafluorophosphate) salt.

1·4PF_6. (33 mg, 0.13 mmol, 10%) ^{1}H NMR (500 MHz, CD_3CN) δ = 9.28 (d, J = 6 Hz, 2 H), 9.23 (d, J = 7 Hz, 2 H), 9.08 (d, J = 7 Hz, 2 H), 8.49–8.40 (m, 6 H), 8.37 (d, J = 7 Hz, 2 H), 7.68–7.60 (m, 4 H), 7.53 (d, J = 8 Hz, 1 H), 7.49 (s, 1 H), 7.44 (d, J = 8 Hz, 1 H), 6.11 (s, 2 H), 6.04 (s, 2 H), 6.02 (s, 2 H), 2.32 (s, 3 H); ^{13}C NMR (125 MHz, CD_3CN) δ = 149.8, 149.5, 145.6, 145.4, 145.3, 145.2, 139.2, 136.4, 136.2, 136.1, 134.4, 132.1, 131.9, 130.4, 130.3, 127.6, 127.3, 127.2, 127.1, 64.6, 64.5, 62.2, 18.2; ESI-HRMS: m/z calcd for $C_{37}H_{34}F_{18}N_4P_3$ $[M - PF_6]^+$ = 1305.3267; found 1305.3134.

2·4PF_6. (150 mg, 0.127 mmol, 18%) ^{1}H NMR (500 MHz, CD_3CN) δ = 9.47 (d, J = 7 Hz, 2 H), 9.38 (m, 4 H), 8.65 (d,

$J = 7$ Hz, 2 H), 8.62 (d, $J = 7$ Hz, 2 H), 8.56 (d, $J = 7$ Hz, 2 H), 8.51 (d, $J = 7$ Hz, 2 H), 8.36 (d, $J = 6$ Hz, 2 H), 7.82–7.74 (m, 6 H), 7.71 (dd, $J = 7$ Hz, 2 Hz, 1 H), 7.62–7.57 (m, 3 H), 7.47–7.42 (m, 2 H), 6.25 (s, 2 H), 6.21 (s, 2 H), 6.19 (s, 2 H), 6.17 (s, 2 H); ^{13}C NMR (125 MHz, CD_3CN) $\delta = 149.8, 149.76, 149.7, 149.6, 149.58, 145.4, 145.2, 145.1, 143.9, 137.9, 136.4, 136.0, 133.5, 133.5, 131.9, 131.3, 130.5, 130.4, 129.5, 129.2, 129.2, 128.6, 127.4, 127.4, 127.3, 126.6, 64.6, 64.5, 64.3, 62.3$; ESI-HRMS: m/z calcd for $C_{42}H_{36}F_{18}N_4P_3$ $[M - PF_6]^+ = 1367.3433$; found 1367.3230.

4·4PF$_6$. (284 mg, 0.241 mmol, 34%) ^{1}H NMR (500 MHz, CD_3CN) δ = 8.97–8.86 (m, 8 H), 8.25–8.18 (m, 6 H), 8.15 (d, $J = 7$ Hz, 2 H), 7.81 (d, $J = 2$ Hz, 1 H), 7.72 (d, $J = 8$ Hz, 1 H), 7.63 (dd, $J = 2$ Hz, 8 Hz, 1 H), 7.57 (s, 4 H), 5.93 (s, 2 H), 5.78 (s, 2 H), 5.77 (s, 2 H), 5.76 (s, 2 H); ^{13}C NMR (125 MHz, CD_3CN) $\delta = 63.6, 63.8, 64.6, 117.3, 124.8, 126.9, 127.2, 127.3, 127.4, 129.6, 130.1, 130.3, 133.4, 134.3, 134.9, 135.8, 135.9, 137.8, 145.1, 145.2, 145.7, 149.3, 149.4, 149.7$; ESI-HRMS: m/z calcd for $C_{36}H_{31}F_{12}N_4P_2$ $[M - 2PF_6]^{2+} = 444.0502$; found 444.0519.

5·4PF$_6$. (95 mg, 0.075 mmol, 25%) ^{1}H NMR (500.1 MHz, CD_3CN) $\delta = 8.87$ (m, 6 H), 8.83 (d, $J = 7$ Hz, 2 H), 8.18 (m, 6 H), 8.11 (d, $J = 7$ Hz, 2 H), 7.62 (dd, $J = 8$ Hz, $J = 1$ Hz, 1 H), 7.53 (s, 4 H), 7.62 (d, $J = 8$ Hz, 1 H), 6.94 (s, $J = 1$ Hz, 1 H), 5.74 (s, 4 H), 5.70 (s, 4 H), 3.74 (s, 3 H); ^{13}C NMR (125 MHz, $CDCl_3$) $\delta = 30.7, 56, 5, 61.4, 65.5, 65.8, 112.8, 118.2, 122.9, 125.2, 127.3, 128.1, 128.2, 131.6, 131.2, 132.9, 136.8, 136.9, 138.8, 146.1, 146.7, 149.9, 150.1, 150.3, 150.4, 159.1$; ESI-HRMS: m/z calcd for $C_{37}H_{36}F_{12}N_4OP_2$ $[M - 2PF_6]^{2+} = 420.1008$; found 420.1007.

10. Compound **8** (0.50 g, 2.7 mmol), *n*-bromosuccinimide (1.01 g, 5.7 mmol), and benzoyl peroxide were added to a solution of CH_2Cl_2 (20 mL). The solution was stirred vigorously under reflux for 1 day in the presence of a sodium lamp. After cooling down to room temperature, the solution was filtered, and the solvent was evaporated off under vacuum. Purification of the residue by column chromatography [SiO_2: MeOH : CH_2Cl_2 (1 : 99)] gave compound **10** as a white solid (650 mg, 1.9 mmol, 70%). ^{1}H NMR (125 MHz, $CDCl_3$) $\delta = 7.53–7.40$ (m, 8H), 4.53 (s, 2H), 4.44 (s, 2H); ^{13}C NMR (125 MHz, $CDCl_3$) $\delta = 31.5, 32.6, 121.7, 128.3, 128.49, 128.8, 130.9, 131.4, 135.3, 137.9, 139.5, 142.4$; ESI-HRMS: m/z calcd for $C_{14}H_{12}Br_2 = 338.9208$; found = 338.9196.

19. 2-(2-(2-Azidoethoxy)ethoxy)ethanol (**18**) (7.0 g, 40 mmol) and Et_3N (4.0 g, 39.5 mmol) were added to dry degassed CH_2Cl_2 (175 mL) and the mixture was left to stir for 1 h. The reaction mixture was cooled down to 0 °C and methacryloyl chloride (4.80 g, 46.3 mmol) was added. The reaction was warmed up slowly to 25 °C and stirred for a further 14 h. The solvent was removed under vacuum, and the resulting mixture was subjected to column chromatography [SiO_2: CH_2Cl_2 : hexane (6.5 : 3.5)]. The fractions containing the product were combined and solvent was removed *in vacuo* to give **19** as a colourless oil (7.7 g, 32 mmol, 68%). ^{1}H NMR ($CDCl_3$, 400 MHz, 25 °C): $\delta = 1.89–1.90$ (dd, $J =$ 1.43 Hz, 3H), 3.33 (t, $J = 4.91$ Hz, 2H), 3.59–3.65 (m, 6H), 3.70 (t, $J = 4.92$ Hz, 2H), 4.25 (t, $J = 4.93$ Hz, 2H), 5.52–5.53 (m, 1H), 6.07–6.08 (m, 1H); ^{13}C NMR ($CDCl_3$, 400 MHz, 25 °C): $\delta = 18.3, 50.7, 63.8, 69.0, 69.2, 70.1, 125.7, 136.1, 167.3$; ESI-HRMS: m/z calcd for $C_{10}H_{17}N_3O_4 = 243.121$; found: 244.128 $[M + H]^+$.

20. A mixture of the monomer **19** (250 mg, 1.02 mmol) and Me_2CO (3 mL) were degassed in a Schlenk flask by six freeze-pump-thaw cycles. This mixture was then injected into another dry Schlenk flask containing CuBr (9.3 mg, 0.065 mmol) and 4,4′-dinonyl-2,2′-dipyridal (DNBB) (20.2 g, 0.049 mmol) and the mixture was left to stir for 10 min. Ethyl 2-bromoisobutyrate (EBIB) (9.5 μL, 0.065 mmol) was then injected into the reaction mixture which was left to stir for 16 h. The reaction mixture was diluted with CH_2Cl_2 then washed with saturated aqueous Na_2CO_3 : EDTA mixture. The organic layer was washed with a saturated NaCl solution, dried ($MgSO_4$), and then precipitated into hexane. The solvent was subsequently removed under vacuum, affording the azide polymer **20** (conversion > 95% det. by ^{1}H NMR spectroscopy); M_n = 39,000; M_w = 55,000 PDI = 1.4 det. by GPC analysis. ^{1}H NMR (CD_2Cl_2, 400 MHz, 25 °C): $\delta = 0.86–1.23$ (m, 3H), 1.82–1.96 (m, 2H), 3.39 (s, 2H), 3.64–3.67 (m, 6H), 4.08 (s, 2H); ^{13}C NMR ($CDCl_3$, 400 MHz, 25 °C): $\delta = 16.4, 44.6, 50.8, 63.9, 68.5, 69.9, 70.5, 177.4$.

21·*n*PF$_6$. A mixture of the azide polymer **20** (25.6 mg, 0.105 mmol) and CBPQT^{4+} alkyne derivative **7**·4PF$_6$ (124.5 g, 0.105 mmol) was added to DMF-d_7 (1 mL) in a dry NMR tube and it was degassed by bubbling Ar through the solution for 2 h. An ^{1}H NMR spectrum of this mixture was recorded at this juncture. CuI (20 mg, 0.105 mmol) was then added to the reaction mixture. The reaction was heated to 60 °C in a sandbath and monitored periodically with ^{1}H NMR spectroscopy. After 24 h, the reaction mixture was cooled and washed with aqueous EDTA. The organic layer was then added dropwise to a saturated NH_4PF_6 solution in H_2O to precipitate out the product. The precipitate was recovered by filtration to afford the **21**·*n*PF_6 copolymer as a crystalline brown solid (145 mg, conversion > 95% by ^{1}H NMR); $M_n = 2.27 \times 10^5$ g mol^{-1} (det. by ^{1}H NMR integration analysis); $M_w = (1.99 \pm 0.14) \times 10^6$ g/mol, $M_n = (1.63 \pm 0.07) \times 10^5$ g mol^{-1}, PDI = 1.5 (± 0.1) (det. by SEC-MALS analysis). ^{1}H NMR (DMF-d_7, 500 MHz, 25 °C): $\delta = 0.78–1.32$ (m), 1.66–1.81(br s), 3.51–3.80 (m), 3.92–4.03 (br s), 4.05–4.20 (br s), 4.62–4.88 (m), 5.55–5.75 (m), 6.12–6.28 (br m), 6.30–6.49 (br s), 7.91–8.12 (m), 8.42–8.49 (m), 8.53–8.83 (m), 9.34–9.78 (br m).

23·4PF$_6$. The dicationic building block **16**·2PF$_6$ (204 mg, 0.289 mmol) was added to a solution of the dibromide **15** (100 mg, 0.289 mmol) and macrocycle **22** (100 mg, 0.135 mmol) dissolved in dry DMF (50 mL). The reaction mixture was stirred for 1 week. The solvent was removed from the resulting green solution under vacuum, and the green solid was redissolved in Me_2CO. The solution was subjected to column chromatography (SiO_2), first eluting the yellow band containing unreacted macrocycle **22** using Me_2CO and then changing to [MeOH/$MeNO_2$/H_2O/2M NH_4Cl (7 : 1 : 2)]. The eluent was removed under vacuum, the solid was dissolved in hot H_2O, and a saturated aqueous solution of NH_4PF_6 was added until no further precipitate was observed. The precipitate was recovered by filtration to afford **23**·4PF_6 (101 mg, 0.052 mmol, 39%) as a green solid. ^{1}H NMR (CD_3CN, 400 MHz, 25 °C): $\delta = 3.02$ (s, 1H), 3.50–4.16 (m, 36H), 5.08 (s, 2H), 5.67 (s, 4H), 5.84 (s, 2H), 5.96 (s, 2H), 6.06 (br s, 2H), 6.69–6.78 (m, 2H), 7.23–7.34 (br s, 4H), 7.38–7.426 (br s, 3 H), 7.57–7.70 (m, 8H), 7.73–7.88 (m, 3H), 8.30–8.42 (s, 1H), 8.54–9.29 (m, 8H); ^{13}C NMR (CD_3CN, 400 MHz, 25 °C): $\delta = 22.7, 28.6, 33.7, 34.5, 38.5, 40.4, 56.7, 61.9, 64.1, 64.6, 64.8, 64.9, 68.0, 68.3, 69.8, 70.0, 70.2, 70.6,$

70.7, 70.8, 71.1, 71.2, 71.5, 106.1, 107.8, 108.0, 114.1, 125.7, 126.3, 130.1, 131.2, 132.8, 134.9, 135.9, 136.6, 144.7, 144.9, 145.2, 154.1, 173.6.; ESI-HRMS: m/z calcd for $C_{74}H_{78}O_{12}N_4P_4S_4F_{24}$: 1922.31; found: 1777.340 $[M - PF_6]^{3+}$, 816.292 $[M - 2PF_6]^{2+}$, 495.843 $[M - 3PF_6]^{+}$, 743.276 $[M - 2PF_6 - HPF_6]^{2+}$.

24·*n*PF$_6$. A mixture of the azide polymer **20** (30 mg, 0.123 mmol) and **23**·4PF$_6$ (63 mg, 0.033 mmol) was added to DMF-d_7 (1 mL) in a dry NMR tube and it was degassed by bubbling Ar through the solution for 2 h. An ^{1}H NMR spectrum of this mixture was taken at this point. CuI (15 mg, 0.079 mmol) was added to the reaction mixture. The reaction mixture was then heated to 60 °C in a sandbath for 24 h, and followed periodically by NMR spectroscopy. Excess of methyl propargyl ether was then injected into the reaction mixture, and heated for an additional 24 h at 60 °C. The reaction mixture was cooled and washed with aqueous EDTA. The organic layer was then added dropwise to a saturated NH_4PF_6 solution in MeOH to precipitate out the product. The precipitate was recovered by filtration to afford the side-chain poly[2]catenane **24**·*n*PF$_6$ as a crystalline green solid (90 mg, conversion > 95% det. by ^{1}H NMR spectroscopy); $M_n = 1.28 \times 10^5$ g mol^{-1} (det. by ^{1}H NMR integration analysis); $M_w = (1.3 \pm 0.07) \times 10^6$ g mol^{-1}, $M_n = (8.7 \pm 0.61) \times 10^5$ g mol^{-1}, PDI =1.5 (± 0.1) (det. by SEC-MALS analysis). ^{1}H NMR (DMF-d_7, 500 MHz, 25 °C): δ = 0.80–1.37 (m), 1.72–2.19 (m), 3.24–4.89 (m), 5.56–5.85 (br s), 5.89–6.27 (m), 6.32–6.57 (br s), 6.75–6.89 (br s), 7.23–7.37 (br s), 7.37–7.47 (br s), 7.69–8.14 (m), 8.20–8.75 (m), 9.12–9.74 (m).

Isothermal titration microcalorimetry

Microcalorimetry was carried out using a Microcal VP-ITC titration microcalorimeter. Aliquouts (3–7 μL) of degassed solutions of the guest in MeCN were titrated with stirring into solutions of the host at 298 K. The heat of dilution for each titration was measured by determining the heat released on the injection of the guest into MeCN in the absence of host, and the enthalpy of dilution was subtracted from the enthalpy of the titration to determine the enthalpy of complexation. Software provided by Microcal LLC was used to compute the thermodynamic parameters of the titration (ΔG°, K_a, ΔS°, ΔH°) based on the one-site binding model. The reported values in Table 1 are the mean results of multiple titrations, and errors are reported as a standard deviation from the mean.

Cyclic voltammetry

Electrochemical experiments were carried out at room termperature in argon-purged solutions of MeCN, with a Gamry Reference 600 potentiostat/galvanostat/ZRA interfaced to a PC. Cyclic voltammetric experiments were perfomed by using a glassy carbon working electrode (0.07 cm^2); its surface was polished routinely with 0.05 mm of alumina–water slurry on a felt surface immediately before each run. The counter electrode was a Pt wire and the reference electrode was a Ag/AgCl electrode. Tetrabutylammonium hexafluorophosphate (0.1 M) was added as a supporting electrolyte.

X-Ray crystal data

23·4PF$_6$. The X-ray crystal data for compound **23·4PF$_6$** was collected at 173 K using a Rigaku MM007 High brilliance RA generator (Cu-K$_\alpha$ radiation) equipped with confocal optics and Saturn92 CCD system. The results were obtained after collecting data for many crystals from different crystallisation attempts. All of the crystals examined gave the same unit cell and crystal system; the data reported here is the most well behaved. Intensities were corrected for Lorentz-polarization and for absorption. The structure was solved by direct methods. Hydrogen atoms bound to carbon were idealised. Structural refinements were obtained with full-matrix least-squares based on F^2 by using the program SHELXTL.[27] CCDC 720651 contains the supplementary crystallographic data for this compound.†

*Crystal data for **23·4PF$_6$**.* $C_{74}H_{78}F_{24}N_4O_{12}P_4S_4.6.5H_2O.C_6H_{14}O$, $M = 2142.80$, space group $P2_1/c$, monoclinic, $a = 14.216(4)$, $b = 54.971(12)$, $c = 13.678(4)$ Å, $\beta = 109.254(7)°$, $U = 10091(4)$ Å^3, $Z = 4$, $\mu = 2.427$ mm^{-1}, 126248 reflections collected, 11023 observed independent reflections (R_{int} 0.0854) gave R 0.1969 for $I > 2\sigma(I)$ and w$R(F^2)$ was 0.5261.

DNP-DEG⊂1·4PF$_6$ and TTF⊂1·4PF$_6$. The X-ray crystal data for DNP-DEG⊂**1**·4PF$_6$ and TTF⊂**1**·4PF$_6$ were collected with a Bruker Smart 1000 CCD-based X-ray diffractometer. The frames for the data collection were integrated with the Bruker SAINT program system using a narrow-frame integration algorithm. The superstructures were solved by direct methods and refined based on F^2 using the SHELXTL software package.[36] CCDC 720652–720653 contain the supplementary crystallographic data for these compounds.†

*Crystal data for DNP-DEG⊂**1**·4PF$_6$.* $C_{67}H_{76}N_{10}O_6](PF_6)_4$, $M = 1697.26$, space group $P2_1/n$, monoclinic, $a = 13.8934(9)$, $b = 23.2237(16)$, $c = 13.0531(9)$ Å, $\beta = 116.2620(10)°$, $V = 3776.9(4)$ Å^3, $Z = 2$, $D_{calcd.} = 1.492$ g cm^{-3}, μ(Mo-K$_\alpha$) = 0.216 mm^{-1}, $T = 120(2)$ K, red prisms, 9064 independent measured reflections, 5614 independent observed reflections [$|F_o| > 4\sigma(|F_o|)$, $2\theta_{max} = 54°$], F^2 refinement, $R_1 = 0.061$, w$R_2 = 0.139$, 538 parameters.

*Crystal data for TTF⊂**1**·4PF$_6$.* $C_{43}H_{38}N_4S_4](PF_6)_4.1.8(C_2H_3N)$ $M = 1392.79$, space group $P2_1/n$, monoclinic, $a = 10.8498(8)$, $b = 19.3989(14)$, $c = 13.8729(10)$ Å, $\beta = 106.5760(10)°$, $V = 2798.5(4)$ Å^3, $Z = 2$, $D_{calcd.} = 1.653$ g cm^{-3}, μ(Mo-K$_\alpha$) = 0.406 mm^{-1}, $T = 120(2)$ K, green block, 6723 independent measured reflections, 4363 independent observed reflections [$|F_o| > 4\sigma(|F_o|)$, $2\theta_{max} = 56°$], F^2 refinement, $R_1 = 0.052$, w$R_2 = 0.137$, 436 parameters.

Acknowledgements

This material is based upon work supported by the National Science Foundation under CHE-0924620. L. F. gratefully acknowledges the support of a Ryan Fellowship from Northwestern University. A. B. B. gratefully acknowledges the support of a NIH Postdoctoral Fellowship (F32CA136148-02).

Notes and references

1 (*a*) P.-L. Anelli, P. R. Ashton, R. Ballardini, V. Balzani, M. Delgado, M. T. Gandolfi, T. T. Goodnow, A. E. Kaifer, D. Philp, M. Pietraszkiewicz, L. Prodi, M. V. Reddington, A. M. Z. Slawin, N. Spencer, J. F. Stoddart, C. Vicent and D. J. Williams, *J. Am. Chem. Soc.*, 1992, **114**, 193–218; (*b*) R. Jager and F. Vögtle, *Angew. Chem., Int.*

Ed. Engl., 1997, **36**, 930–944; (*c*) F. Aricó, J. D. Badjić, S. J. Cantrill, A. H. Flood, K. C.-F. Leung, Y. Liu and J. F. Stoddart, *Top. Curr. Chem.*, 2005, **249**, 203–259; (*d*) J. F. Stoddart and H. M. Colquhoun, *Tetrahedron*, 2008, **64**, 8231–8263.

2 (*a*) G. Schill, *Catenanes, Rotaxanes and Knots*, Academic Press, New York, 1971; (*b*) *Molecular Catenanes, Rotaxanes and Knots*, ed. J.-P. Sauvage, C.O. Dietrich-Buchecker, Wiley-VCH, Weinheim, 1999.

3 (*a*) P.-L. Anelli, N. Spencer and J. F. Stoddart, *J. Am. Chem. Soc.*, 1991, **113**, 5131–5133; (*b*) P. R. Ashton, R. Górski, D. Philp, N. Spencer, J. F. Stoddart and M. S. Tolley, *Synlett*, 1992, 914–918; (*c*) P. R. Ashton, R. Górski, D. Philp, N. Spencer, J. F. Stoddart and M. S. Tolley, *Synlett*, 1992, 919–922; (*d*) P. R. Ashton, R. A. Bissell, N. Spencer, J. F. Stoddart and M. S. Tolley, *Synlett*, 1992, 923–926; (*e*) P. R. Ashton, D. Philp, N. Spencer and J. F. Stoddart, *J. Chem. Soc., Chem. Commun.*, 1992, 1124–1128; (*f*) P.-L. Anelli, M. Asakawa, P. R. Ashton, R. A. Bissell, G. Clavier, R. Górski, A. E. Kaifer, S. J. Langford, G. Mattersteig, S. Menzer, D. Philp, A. M. Z. Slawin, N. Spencer, J. F. Stoddart, M. S. Tolley and D. J. Williams, *Chem.–Eur. J.*, 1997, **3**, 1113–1135; (*g*) J. Cao, M. C. T. Fyfe, J. F. Stoddart, G. R. L. Cousins and P. T. Glink, *J. Org. Chem.*, 2000, **65**, 1937–1946; (*h*) S. J. Loeb and J. A. Wisner, *Chem. Commun.*, 2000, 1939–1940; (*i*) D. A. Leigh, A. Troisi and F. Zerbetto, *Angew. Chem., Int. Ed.*, 2000, **39**, 350–353; (*j*) M. Bělohradský, A. M. Elizarov and J. F. Stoddart, *Collect. Czech. Chem. Commun.*, 2002, **67**, 1719–1728; (*k*) K. Hirose, Y. Shiba, K. Ishibashi, Y. Doi and Y. Tobe, *Chem.–Eur. J.*, 2008, **14**, 3427–3433; (*l*) I. Yoon, D. Benítez, Y.-L. Zhao, O. Š. Miljanić, S.-Y. Kim, E. Tkatchouk, K. C.-F. Leung, S. I. Khan, W. A. III Goddard and J. F. Stoddart, *Chem.–Eur. J.*, 2009, **15**, 1115–1122.

4 (*a*) R. A. Bissell, E. Córdova, A. E. Kaifer and J. F. Stoddart, *Nature*, 1994, **369**, 133–137; (*b*) M. Asakawa, P. R. Ashton, V. Balzani, A. Credi, C. Hamers, G. Mattersteig, M. Montalti, A. N. Shipway, N. Spencer, J. F. Stoddart, M. S. Tolley, M. Venturi, A. J. P. White and D. J. Williams, *Angew. Chem., Int. Ed.*, 1998, **37**, 333–337; (*c*) J. O. Jeppesen, J. Perkins, J. Becher and J. F. Stoddart, *Angew. Chem., Int. Ed.*, 2001, **40**, 1216–1221; (*d*) H.-R. Tseng, S. A. Vignon and J. F. Stoddart, *Angew. Chem., Int. Ed.*, 2003, **42**, 1491–1495; (*e*) H.-R. Tseng, S. A. Vignon, P. C. Celestre, J. Perkins, J. O. Jeppesen, A. Di Fabio, R. Ballardini, M. T. Gandolfi, M. Venturi, V. Balzani and J. F. Stoddart, *Chem.–Eur. J.*, 2004, **10**, 155–172; (*f*) I. Aprahamian, T. Yasuda, T. Ikeda, S. Saha, W. R. Dichtel, K. Isoda, T. Kato and J. F. Stoddart, *Angew. Chem., Int. Ed.*, 2007, **46**, 4675–4679; (*g*) I. Aprahamian, W. R. Dichtel, T. Ikeda, J. R. Heath and J. F. Stoddart, *Org. Lett.*, 2007, **9**, 1287–1290; (*h*) Y.-L. Zhao, I. Aprahamian, A. Trabolsi, N. Erina and J. F. Stoddart, *J. Am. Chem. Soc.*, 2008, **130**, 6348–6350; (*i*) Y.-L. Zhao, W. R. Dichtel, A. Trabolsi, S. Saha, I. Aprahamian and J. F. Stoddart, *J. Am. Chem. Soc.*, 2008, **130**, 11294–11296; (*j*) I. Aprahamian, J. C. Olsen, A. Trabolsi and J. F. Stoddart, *Chem.–Eur. J.*, 2008, **14**, 3889–3895.

5 (*a*) C. P. Collier, E. W. Wong, M. Bělohradský, F. M. Raymo, J. F. Stoddart, P. J. Kuekes, R. S. Williams and J. R. Heath, *Science*, 1999, **285**, 391–394; (*b*) C. P. Collier, G. Mattersteig, E. W. Wong, Y. Luo, K. Beverly, J. Sampaio, F. M. Raymo, J. F. Stoddart and J. R. Heath, *Science*, 2000, **289**, 1172–1175; (*c*) Y. H. Jang, S. G. Hwang, Y. H. Kim, S. S. Jang and W. A. Goddard, *J. Am. Chem. Soc.*, 2004, **126**, 12636–12645; (*d*) A. H. Flood, J. F. Stoddart, D. W. Steuerman and J. R. Heath, *Science*, 2004, **306**, 2055–2056; (*e*) K. Nørgaard, B. W. Laursen, S. Nygaard, K. Kjaer, H.-R. Tseng, A. H. Flood, J. F. Stoddart and T. Bjørnholm, *Angew. Chem., Int. Ed.*, 2005, **44**, 7035–7039; (*f*) Y. H. Jang and W. A. Goddard, *J. Phys. Chem. B*, 2006, **110**, 7660–7665; (*g*) A. H. Flood, E. W. Wong and J. F. Stoddart, *Chem. Phys.*, 2006, **324**, 280–290; (*h*) R. Beckman, K. Beverly, A. Boukai, Y. Bunimovich, J. W. Choi, E. DeIonno, J. Green, E. Johnston-Halperin, Y. Luo, B. Sheriff, J. F. Stoddart and J. R. Heath, *Faraday Discuss.*, 2006, **131**, 9–22; (*i*) J. E. Green, J. W. Choi, A. Boukai, Y. Bunimovich, E. Johnston-Halperin, E. DeIonno, Y. Luo, B. A. Sheriff, K. Xu, Y. S. Shin, H.-R. Tseng, J. F. Stoddart and J. R. Heath, *Nature*, 2007, **445**, 414–417; (*j*) W. R. Dichtel, J. R. Heath and J. F. Stoddart, *Philos. Trans. R. Soc. London, Ser. A*, 2007, **365**, 1607–1625; (*k*) V. Balzani, A. Credi and M. Venturi, *Molecular Devices and Machinery: Concepts and Perspectives for the Nanoworld*, Wiley-VCH, Weinheim, 2008.

6 For references on nanoswitches, molecular actuators, and molecular nanovalves see: (*a*) V. Balzani, A. Credi, F. M. Raymo and J. F. Stoddart, *Angew. Chem. Int. Ed.*, 2000, **39**, 3348–3391; (*b*) R. Ballardini, V. Balzani, A. Credi, M. T. Gandolfi and M. Venturi, *Acc. Chem. Res.*, 2001, **34**, 445–455; (*c*) J. P. Collin, C. Dietrich-Buchecker, P. Gavina, M.-C. Jimenez-Molero and J.-P. Sauvage, *Acc. Chem. Res.*, 2001, **34**, 477–487; (*d*) A. Hanke and R. Metzler, *Chem. Phys. Lett.*, 2002, **359**, 22–26; (*e*) A. H. Flood, R. J. A. Ramírez, W. Q. Deng, R. P. Muller, W. A. Goddard and J. F. Stoddart, *Aust. J. Chem.*, 2004, **57**, 301–322; (*f*) T. D. Nguyen, H.-R. Tseng, P. C. Celestre, A. H. Flood, Y. Liu, J. F. Stoddart and J. I. Zink, *Proc. Natl. Acad. Sci. U. S. A.*, 2005, **102**, 10029–10034; (*g*) S. Bonnet, J. P. Collin, M. Koizumi, P. Mobian and J.-P. Sauvage, *Adv. Mater.*, 2006, **18**, 1239–1250; (*h*) E. R. Kay, D. A. Leigh and F. Zerbetto, *Angew. Chem., Int. Ed.*, 2007, **46**, 72–191; (*i*) S. Saha, K. C.-F. Leung, T. D. Nguyen, J. F. Stoddart and J. I. Zink, *Adv. Funct. Mater.*, 2007, **17**, 685–693; (*j*) T. D. Nguyen, Y. Liu, S. Saha, K. C.-F. Leung, J. F. Stoddart and J. I. Zink, *J. Am. Chem. Soc.*, 2007, **129**, 626–634; (*k*) V. Balzani, A. Credi and M. Venturi, *ChemPhysChem*, 2008, **9**, 202–220; (*l*) K. Patel, S. Angelos, W. R. Dichtel, A. Coskun, Y.-W. Yang, J. I. Zink and J. F. Stoddart, *J. Am. Chem. Soc.*, 2008, **130**, 2382–2383; (*m*) S. Angelos, Y.-W. Yang, K. Patel, J. F. Stoddart and J. I. Zink, *Angew. Chem., Int. Ed.*, 2008, **47**, 2222–2226.

7 (*a*) T. J. Huang, B. Brough, C.-M. Ho, Y. Liu, A. H. Flood, P. A. Bonvallet, H.-R. Tseng, J. F. Stoddart, M. Baller and S. Magonov, *Appl. Phys. Lett.*, 2004, **85**, 5391–5393; (*b*) T. J. Huang, H.-R. Tseng, L. Sha, W. X. Lu, B. Brough, A. H. Flood, B. D. Yu, P. C. Celestre, J. P. Chang, J. F. Stoddart and C.-M. Ho, *Nano Lett.*, 2004, **4**, 2065–2071; (*c*) T. J. Huang, A. H. Flood, B. Brough, Y. Liu, P. A. Bonvallet, S. S. Kang, C. W. Chu, T. F. Guo, W. X. Lu, Y. Yang, J. F. Stoddart and C.-M. Ho, *IEEE Transactions on Automation Science and Engineering*, 2006, **3**, 254–259.

8 (*a*) V. Bermudez, N. Capron, T. Gase, F. G. Gatti, F. Kajzar, D. A. Leigh, F. Zerbetto and S. W. Zhang, *Nature*, 2000, **406**, 608–611; (*b*) J. D. Badjić, V. Balzani, A. Credi, J. N. Lowe, S. Silvi and J. F. Stoddart, *Chem.–Eur. J.*, 2004, **10**, 1926–1935; (*c*) Y. Sowa, A. D. Rowe, M. C. Leake, T. Yakushi, M. Homma, A. Ishijima and R. M. Berry, *Nature*, 2005, **437**, 916–919; (*d*) W. Wang and A. E. Kaifer, *Angew. Chem., Int. Ed.*, 2006, **45**, 7042–7046; (*e*) S. Nygaard, B. W. Laursen, A. H. Flood, C. N. Hansen, J. O. Jeppesen and J. F. Stoddart, *Chem. Commun.*, 2006, 144–146; (*f*) C. A. Nijhuis, B. J. Ravoo, J. Huskens and D. N. Reinhoudt, *Coord. Chem. Rev.*, 2007, **251**, 1761–1780; (*g*) J. W. Lee, I. Hwang, W. S. Jeon, Y. H. Ko, S. Sakamoto, K. Yamaguchi and K. Kim, *Chem.–Asian J.*, 2008, **3**, 1277–1283.

9 (*a*) W. S. Jeon, A. Y. Ziganshina, J. W. Lee, Y. H. Ko, J. K. Kang, C. Lee and K. Kim, *Angew. Chem., Int. Ed.*, 2003, **42**, 4097–4100; (*b*) P. Mobian, J. M. Kern and J.-P. Sauvage, *Angew. Chem., Int. Ed.*, 2004, **43**, 2392–2395; (*c*) Y. Norikane and N. Tamaoki, *Org. Lett.*, 2004, **6**, 2595–2598; (*d*) J. Berna, D. A. Leigh, M. Lubomska, S. M. Mendoza, E. M. Perez, P. Rudolf, G. Teobaldi and F. Zerbetto, *Nat. Mater.*, 2005, **4**, 704–710; (*e*) F. M. Raymo, *Angew. Chem., Int. Ed.*, 2006, **45**, 5249–5251; (*f*) A. Credi, *Aust. J. Chem.*, 2006, **59**, 157–169; (*g*) B. Champin, P. Mobian and J.-P. Sauvage, *Chem. Soc. Rev.*, 2007, **36**, 358–366; (*h*) S. Bonnet and J. P. Collin, *Chem. Soc. Rev.*, 2008, **37**, 1207–1217.

10 (*a*) A. H. Flood, A. J. Peters, S. A. Vignon, D. W. Steuerman, H.-R. Tseng, S. Kang, J. R. Heath and J. F. Stoddart, *Chem.–Eur. J.*, 2004, **10**, 6558–6564; (*b*) J. O. Jeppesen, S. Nygaard, S. A. Vignon and J. F. Stoddart, *Eur. J. Org. Chem.*, 2005, 196–220; (*c*) J. W. Choi, A. H. Flood, D. W. Steuerman, S. Nygaard, A. B. Braunschweig, N. N. P. Moonen, B. W. Laursen, Y. Luo, E. Delonno, A. J. Peters, J. O. Jeppesen, K. Xu, J. F. Stoddart and J. R. Heath, *Chem.–Eur. J.*, 2006, **12**, 261–279.

11 (*a*) J.-M. Lehn, *Supramolecular Chemistry*, VCH, New York, 1995; (*b*) *Comprehensive Supramolecular Chemistry*, ed. J. L. Atwood, J. E. D. Davies, D. D. MacNicol, F. Vögtle and J.-M. Lehn, Pergamon Press, Oxford, 1996, vol. 2; (*c*) F. L. Lindoy and I. M. Atkinson, *Self-Assembly in Supramolecular Systems, Monographs in Supramolecular Chemistry*, series ed. J. F. Stoddart, Royal Society of Chemistry, Cambridge, 2000; (*d*) H.-J. Schneider and A. Yatsimirsky, *Principles and Methods in Supramolecular Chemistry*, Wiley, Chichester, 2000.

12 J. M. Timko, R. C. Helgeson, M. Newcomb, G. W. Gokel and D. J. Cram, *J. Am. Chem. Soc.*, 1974, **96**, 7097–7099.

13 D. J. Cram and J. M. Cram, *Container Molecules and their Guests, Monographs in Supramolecular Chemistry*, series ed. J. F. Stoddart, Royal Society of Chemistry, Cambridge, 1994.

14 (*a*) P. R. Ashton, D. Philp, N. Spencer and J. F. Stoddart, *J. Chem. Soc., Chem. Commun.*, 1991, 1677–1679; (*b*) P. R. Ashton, D. Philp, M. V. Reddington, A. M. Z. Slawin, N. Spencer, J. F. Stoddart and D. J. Williams, *J. Chem. Soc., Chem. Commun.*, 1991, 1680–1683; (*c*) P.-L. Anelli, P. R. Ashton, N. Spencer, A. M. Z. Slawin, J. F. Stoddart and D. J. Williams, *Angew. Chem., Int. Ed. Engl.*, 1991, **30**, 1036–1039; (*d*) P. R. Ashton, P. T. Glink, M.-V. Martínez-Díaz, J. F. Stoddart, A. J. P. White and D. J. Williams, *Angew. Chem., Int. Ed.*

Engl., 1996, **35**, 1930–1933; (*e*) B. H. Northrop, S. I. Kahn and J. F. Stoddart, *Org. Lett.*, 2006, **8**, 2159–2162.
15 (*a*) K. N. Houk, S. Menzer, S. P. Newton, F. M. Raymo, J. F. Stoddart and D. J. Williams, *J. Am. Chem. Soc.*, 1999, **121**, 1479–1487; (*b*) F. M. Raymo, M. D. Bartberger, K. N. Houk and J. F. Stoddart, *J. Am. Chem. Soc.*, 2001, **123**, 9264–9267; (*c*) M. Venturi, S. Dumas, V. Balzani, J. Cao and J. F. Stoddart, *New J. Chem.*, 2004, **28**, 1032–1037.
16 (*a*) R. Castro, K. R. Nixon, J. D. Evanseck and A. E. Kaifer, *J. Org. Chem.*, 1996, **61**, 7298–7303; (*b*) M. R. Bryce, G. Cooke, F. M. A. Duclairoir and V. M. Rotello, *Tetrahedron Lett.*, 2001, **42**, 1143–1145; (*c*) M. B. Nielsen, J. O. Jeppesen, J. Lau, C. Lomholt, D. Damgaard, J. P. Jacobsen, J. Becher and J. F. Stoddart, *J. Org. Chem.*, 2001, **66**, 3559–3563; (*d*) A. B. Braunschweig, B. N. Northrop and J. F. Stoddart, *J. Mater. Chem.*, 2006, **16**, 32–44.
17 (*a*) Y. Liu, A. H. Flood, P. A. Bonvallet, S. A. Vignon, B. Northrop, H.-R. Tseng, J. Jeppesen, T. J. Huang, B. Brough, M. Baller, S. Magonov, S. Solares, W. A. III, Goddard, C.-M. Ho and J. F. Stoddart, *J. Am. Chem. Soc.*, 2005, **127**, 9745–9759; (*b*) R. Klajn, L. Fang, A. Coskun, M. A. Olson, P. J. Wesson, J. F. Stoddart and B. A. Grzybowski, *J. Am. Chem. Soc.*, 2009, **131**, 4233–4235.
18 M. Hibert and G. Solladie, *J. Org. Chem.*, 1980, **45**, 4496–4498.
19 A. C. Benniston and A. Harriman, *Synlett*, 1993, 223–226.
20 T. J. Katz, A. Sudhakar, M. F. Teasley, A. M. Gilbert, W. E. Geiger, M. P. Robben, M. Wuensch and M. D. Ward, *J. Am. Chem. Soc.*, 1993, **115**, 3182–3198.
21 P. Wipf and J.-K. Jung, *J. Org. Chem.*, 2000, **65**, 6319–6337.
22 (*a*) B. S. Sumerlin, N. V. Tsarevsky, G. Louche, R. Y. Lee and K. Matyjaszewski, *Macromolecules*, 2005, **38**, 7540–7545; (*b*) N. V. Tsarevsky, B. S. Sumerlin and K. Matyjaszewski, *Macromolecules*, 2005, **38**, 3558–3561; (*c*) H. Gao and K. Matyjaszewski, *J. Am. Chem. Soc.*, 2007, **129**, 6633–6639; (*d*) J. Zhang, Y. Zhou, Z. Zhu, Z. Ge and S. Liu, *Macromolecules*, 2008, **41**, 1444–1454.
23 T. R. Chan, R. Hilgraf, K. B. Sharpless and V. V. Fokin, *Org. Lett.*, 2004, **6**, 2853–2855.
24 (*a*) P. J. Wyatt, *Anal. Chim. Acta*, 1993, **272**, 1–40; (*b*) *Handbook of Size Exclusion Chromatography and Related Techniques* ed. C. Wu, Marcel Dekker, New York, 2004.
25 (*a*) R. Huisgen, G. Szeimies and L. Möbius, *Chem. Ber.*, 1967, **100**, 2494–2507; (*b*) J. Bastide, J. Hamelin, F. Texier and V. Q. Ven, *Bull. Chim. Soc. Fr.*, 1973, 2555–2579 and 2871–2887; (*c*) R. Huisgen, *Pure Appl. Chem.*, 1989, **61**, 613–628; (*d*) H. C. Kolb, M. G. Finn and K. B. Sharpless, *Angew. Chem., Int. Ed.*, 2001, **40**, 2004–2021; (*e*) V. V. Rostovtsev, L. G. Green, V. V. Folkin and K. B. Sharpless, *Angew. Chem., Int. Ed.*, 2002, **41**, 2596–2599; (*f*) C. W. Tornoe, C. Christensen and M. Meldal, *J. Org. Chem.*, 2002, **67**, 3057–3064; (*g*) W. R. Dichtel, O. Š. Miljanić, J. M. Spruell, J. R. Heath and J. F. Stoddart, *J. Am. Chem. Soc.*, 2006, **128**, 10388–10390; (*h*) O. Š. Miljanić, W. R. Dichtel, S. Mortezaei and J. F. Stoddart, *Org. Lett.*, 2006, **8**, 4835–4838; (*i*) A. B. Braunschweig, W. R. Dichtel, O. Š. Miljanić, M. A. Olson, J. M. Spruell, S. I. Khan, J. R. Heath and J. F. Stoddart, *Chem.–Asian J.*, 2007, **2**, 634–647; (*j*) J. M. Spruell, W. R. Dichtel, J. R. Heath and J. F. Stoddart, *Chem.–Eur. J.*, 2008, **14**, 4168–4177.
26 The thermodynamic parameters (ΔH°, ΔS°, ΔG°_{298K}, K_a) obtained by isothermal titration microcalorimetry are a result of direct measurement of the heat of reaction (ΔH°) for the threading process of pseudorotaxane formation. A 0.39 mM standard solution for all $CBPQT^{4+}$ derivatives was used for all titrations into which solutions of various concentrations of guest were added in 5 μL aliquots (4.7 mM TTF, 3.2 mM TTF-DEG; 3.9 mM DNP-DEG). Fits were performed using Microcal LLC software. The stoichiometry of all complexes was between 0.99 and 1.02 indicating a 1 : 1 complex is formed.
27 (*a*) L. P. Hammett, *J. Am. Chem. Soc.*, 1937, **59**, 96–103; (*b*) C. Hansch and A. Leo, *Substituent Constants for Correlation Analysis in Chemistry and Biology*, Wiley-Interscience, New York, 1979; (*c*) C. Hansch, A. Leo and R. W. Taft, *Chem. Rev.*, 1991, **91**, 165–195.
28 (*a*) S. Winstein and N. J. Holness, *J. Am. Chem. Soc.*, 1955, **77**, 5562–5578; (*b*) E. L. Eliel, S. H. Wilen and L. N. Mander, *Stereochemistry of Organic Compounds*, John Wiley & Sons, New York, 1994.
29 (*a*) R. W. Taft, *J. Am. Chem. Soc.*, 1952, **74**, 3120–3128; (*b*) R. W. Taft in, *Steric Effects in Organic Chemistry*, series ed. M. S. Newman, John Wiley & Sons, New York, 1956.
30 (*a*) S. S. Jang, Y. H. Jang, Y.-H. Kim, W. A. III Goddard, A. H. Flood, B. W. Laursen, H.-R. Tseng, J. F. Stoddart, J. O. Jeppesen, J. W. Choi, D. W. Steuerman, E. DeIonno and J. R. Heath, *J. Am. Chem. Soc.*, 2005, **127**, 1563–1575; (*b*) H. Kim, W. A. Goddard, S. S. Jang, W. R. Dichtel, J. R. Heath and J. F. Stoddart, *J. Phys. Chem. A*, 2009, **113**, 2136–2143.
31 M. A. Olson, A. B. Braunschweig, L. Fang, T. Ikeda, R. Klajn, A. Trabolsi, P. J. Wesson, D. Benitez, C. A. Mirkin, B. A. Grzybowski and J. F. Stoddart, *Angew. Chem., Int. Ed.*, 2009, **48**, 1792–1797.
32 (*a*) D. H. Busch and N. A. Stephenson, *Coord. Chem. Rev.*, 1990, **100**, 119–154; (*b*) H. L. Anderson, S. Anderson and J. K. M. Sanders, *Acc. Chem. Res.*, 1993, **26**, 469–475; (*c*) J. F. Stoddart and H.-R. Tseng, *Proc. Natl. Acad. Sci. U. S. A.*, 2002, **99**, 4797–4800; (*d*) M. J. Blanco, J. C. Chambron, M. C. Jiménez and J.-P. Sauvage, *Top. Stereochem.*, 2002, **23**, 125–173; (*e*) D. H. Busch, *Top. Curr. Chem.*, 2005, **249**, 1–65; (*f*) *Templated Organic Synthesis* ed. F. Diederich, P. J. Stang, Wiley-VCH, Weinheim, 2006; (*g*) K. E. Griffiths and J. F. Stoddart, *Pure Appl. Chem.*, 2008, **80**, 485–506.
33 Although the UV-vis plots illustrate a large number of data points from which to calculate thermodynamics using a van't Hoff plot, a subset of these data points were chosen correlating to temperatures in which an isosbestic point can be observed for the overlapping spectra. Choosing this subset of data points insures that the temperature range used is one in which the CT at 812 nm ($TTF\subset CBPQT^{4+}$) decreases simultaneously with the increase of the CT band at 475 nm ($DNP\subset CBPQT^{4+}$) in DMF, and that the translation of the host ring is occurring.
34 S. N. Balasubrahmanyam, *Curr. Sci.*, 2008, **94**, 1650–1658.
35 O. Exner, *Nature*, 1962, **196**, 890–891.
36 G. M. Sheldrick, *Acta Crystallogr., Sect. A: Found. Crystallogr.*, 2007, **64**, 112–122.